INTERNATIONAL JOURNAL FOR NUMERICAL METHODS IN ENGINEERING
Int. J. Numer. Meth. Engng. **45**, 251–288 (1999)

REPRODUCING KERNEL HIERARCHICAL PARTITION OF UNITY, PART I—FORMULATION AND THEORY

SHAOFAN LI AND WING KAM LIU*

Department of Mechanical Engineering, Northwestern University, 2145 Sheridan Road, Evanston, IL 60208, U.S.A.

SUMMARY

This work is concerned with developing the hierarchical basis for meshless methods. A reproducing kernel hierarchical partition of unity is proposed in the framework of continuous representation as well as its discretized counterpart. To form such hierarchical partition, a class of basic wavelet functions are introduced. Based upon the built-in consistency conditions, the differential consistency conditions for the hierarchical kernel functions are derived. It serves as an indispensable instrument in establishing the interpolation error estimate, which is theoretically proven and numerically validated. For a special interpolant with different combinations of the hierarchical kernels, a synchronized convergence effect may be observed. Being different from the conventional Legendre function based p-type hierarchical basis, the new hierarchical basis is an intrinsic pseudo-spectral basis, which can remain as a partition of unity in a local region, because the discrete wavelet kernels form a 'partition of nullity'. These newly developed kernels can be used as the multi-scale basis to solve partial differential equations in numerical computation as a p-type refinement. Copyright © 1999 John Wiley & Sons, Ltd.

KEY WORDS: meshless hierarchical partition of unity; wavelet methods; moving least-squares interpolant; reproducing kernel particle method; synchronized convergence

1. INTRODUCTION

In the recent development of meshless methods (see: [1, 2] for survey), several authors have proposed various meshless hierarchical interpolants aiming at efficient and large-scale computations, see e.g. [3–6]. Among them, most notably, are the h–p clouds method by Duarte and Oden [4] and the partition of unity method by Melenk and Babuška [3]. This class of meshless hierarchical shape functions possess some special technical merits:

* Correspondence to: Wing Kam Liu, Department of Mechanical Engineering, Northwestern University, 2145 Sheridan Road, Evanston, IL 60208, U.S.A. E-mail: w-liu@nwu.edu

Contract/grant sponsor: Office of Naval Research
Contract/grant sponsor: Army Research office
Contract/grant sponsor: National Science Foundation
Contract/grant sponsor: Tull Family Endowment Fund
Contract/grant sponsor: Northwestern University
Contract/grant sponsor: Army High Performance Computing Research Center; Contract/grant number: DAAH04-95-2-003/DAAH04-95-C-0008

CCC 0029–5981/99/150251–38$17.50

Received 24 February 1998
Revised 7 July 1998

(i) As the name suggested, they are meshless interpolants, and subsequently the formidable task of mesh generation is relieved.
(ii) They can be conveniently employed in p or h–p adaptive refinement process to obtain highly accurate numerical solutions.
(iii) They provide a suitable basis to support multi-level iterative solvers, which can speed large scale numerical simulations in many computational environment, such as parallel computing.

Note that the term 'hierarchical' used in this paper is strictly in the sense of Zienkiewicz [7], that is: if $\mathbf{u}$ is an unknown function and its approximation is

$$\mathbf{u} \approx \tilde{\mathbf{u}} = \sum_{i=1}^{n} \mathbf{N}_i \mathbf{a}_i$$

then the approximation is hierarchical if an increase of n to $n+1$ does not alter the shape function $\mathbf{N}_i$, $i = 1, \ldots, n$.†

In this paper, a new meshless hierarchical partition of unity is constructed, which is a natural extension of the former moving least-squares (MLS) interpolant by Lancaster and Salkauskas [9], and the recent reproducing kernel interpolant by Liu *et al.* [10]. By taking the original MLS interpolant as the fundamental basis, the hierarchical partition of unity is constructed by adding a sequence of wavelet-like frames, which are the discretization of basic wavelet functions (or mother wavelets) over a random particle distribution. By viewing the interpolation as a sampling, or filtering process, the resulting higher order pseudo-spectral (PS) basis is literally a *wavelet function packet*, meaning that they are are a group of kernel functions with different bandwidth (or support size) in frequency domain, or with different wave number in physical space. That is the root of the term 'wave packet' in physics (e.g. [11]). It also shares the similarity with the specific '*wavelet packets*' in harmonic, and wavelet analysis, such as those proposed by Coifman and Meyer [12], and Chui and Li [13] via multiresolution analysis (MRA) in physical space, or those proposed by Duval-Destin *et al.* [14] in frequency domain.

The authors would like to caution readers that there are subtle differences in the meanings of some technical terms used here. For instance, a hierarchical partition of unity is not equivalent to a hierarchical basis. In this particular context, the hierarchical partition of unity is only a frame in a global sense. There is a difference between wavelet frame and wavelet basis. The former is an 'overcomplete' basis with redundancy, in our case it comes from the discretization of a continuous wavelet transformation; and the latter is usually referred to as a dilation/translation sequence of an $\mathscr{R}$-wavelet. Moreover, the focus of this paper is on the finite-dimensional function space in a bounded region, and usually a wavelet basis in a finite-dimensional space is not a basis in $L^2(\Omega)$. Of course, in good faith, we believe that as the dilation parameter $\rho \to 0$, it will provide a wavelet basis for $L^2(\Omega)$. It may be noted that the wavelet functions employed in the construction of the hierarchical basis are actually the basic, or mother wavelet function by the definition of continuous wavelet transformation, which may or may not form a dyadic wavelet basis, or in general, a $\mathscr{R}$-wavelet basis in $L^2(\Omega)$ (see [15]), though in most cases they may form a non-orthogonal wavelet (pre-wavelet) basis if proper provisions are mandated. Since the main objective of this paper is to construct a meshless hierarchical partition of unity over scattered data, no attempt has been made to construct a new type of dyadic wavelet basis.

† There are other usages of the term 'hierarchical', such as the hierarchical bases in a sense of direct sum of orthogonal subspaces, see e.g. [8]

A complete construction procedure is presented in Section 2 with both continuous and discrete formulations. The built-in global consistency conditions for interpolant kernel are discussed in detail, from which a set of global differential consistency conditions are derived. Aided by these differential consistency conditions, a global interpolation estimate is given. In addition, an interesting synchronized convergence phenomenon is observed, if certain interpolation schemes are adopted. In Section 3, several examples are given to illustrate the construction procedure and their intrinsic properties. Here, the emphasis is placed on how to generate the wavelet-like frame, a partition of nullity, so to speak. It is worthwhile noting that adding a partition of nullity to a partition of unity will result a hierarchical partition of unity; this is in contrast with the Legendre function based p-type hierarchical finite element interpolation scheme [17], which does not form a partition of unity in general. A systematic approximation theory of the proposed hierarchical partition of unity is presented in Section 4. The structures of the basic wavelet functions are further analysed in details in Section 5.

2. FORMULATIONS

To begin with, we formulate a generalized moving least-squares reproducing kernel interpolant via continuous representation. By doing so, a class of hierarchical kernel functions are derived explicitly. Then, its discrete counterpart is formulated by direct discretization of the continuous formulation.

2.1. Generalized moving least-squares reproducing kernel

As shown in [10], a local least-squares approximation of a continuous function, $u(x) \in C^0(\Omega)$, may be expressed as

$$L_{\bar{x}} u(x) := \mathbf{P}\left(\frac{x-\bar{x}}{\varrho}\right) \mathbf{d}(\bar{x}), \quad \forall \bar{x} \in \Omega \tag{1}$$

where $\mathbf{P}$ is a polynomial basis with order m, and $\mathbf{d}$ is an unknown vector. Without loss of generality, the polynomial basis is assumed to have ℓ terms, namely,

$$\mathbf{P}(x) := (P_1, \ldots, P_i, \ldots, P_\ell), \quad P_i(x) \in \pi_m(\Omega) \tag{2}$$

with $P_1 = 1$; $P_i(0) = 0$, $i \neq 1$, where $\pi_m(\Omega)$ denotes the collection of polynomials in $\Omega \subset \mathbb{R}^n$ of total degree $\leqslant m$. The unknown vector $\mathbf{d}(\bar{x})$ can be solved in the moving least-squares procedure, and subsequently equation (1) can be rewritten as [10]

$$L_{\bar{x}} u(x) = \mathbf{P}\left(\frac{x-\bar{x}}{\varrho}\right) \mathbf{M}^{-1}(\bar{x}) \int_{\Omega_y} \mathbf{P}^t \left(\frac{y-\bar{x}}{\varrho}\right) u(y) \phi_\varrho(y-\bar{x}) \, \mathrm{d}\Omega_y \tag{3}$$

where $\phi_\varrho(x) = (1/\varrho^n)\phi(x/\varrho)$ is the weighting function in the least-squares procedure, which we refer to as the window function; $\mathbf{M}$ is the moment matrix,

$$\mathbf{M}(x) := \int_{\Omega_y} \mathbf{P}^t \left(\frac{y-x}{\varrho}\right) \mathbf{P}\left(\frac{y-x}{\varrho}\right) \phi_\varrho(y-x) \, \mathrm{d}\Omega_y \tag{4}$$

Remark 2.1. In formula (3), the components of the polynomial vector $\mathbf{P}(x)$ can be any independent polynomial functions. In fact, the requirement of the polynomials is also not essential.

The construction can be further generalized to include general linearly independent functions as basis, such as trigonometric functions, hyperbolic functions, and any other orthogonal or non-orthogonal basis functions.

So far, all steps followed the moving least-squares reproducing procedure. To construct the new interpolant, instead of assigning the local approximation as what MLS does [9], i.e.

$$u^{\ell}(x,\bar{x}) := L_{\bar{x}}u(x) \tag{5}$$

we propose a different local approximation. Let

$$P_i(x) = \left(\frac{x-\bar{x}}{\varrho}\right)^{\alpha}, \quad 0 \leqslant |\alpha| \leqslant m, \ \ 1 \leqslant i \leqslant \ell \tag{6}$$

with $P_1 = 1$ and $P_\ell(x) = ((x-\bar{x})/\rho)^{\mu}, |\mu| = m$.

Note that there is a relationship between the polynomial order m and the rank of the polynomial vector $\mathbf{P}$, ℓ. Let n denote the dimension of space. $n=1$: $\ell = m+1, n=2$: $\ell = (m+1)(m+2)/2$, and $n=3$: $\ell = (m+1)(m+2)(m+3)/6$. Define

$$\begin{aligned} u^{\ell}(x,\bar{x}) &:= \sum_{|\alpha| \leqslant m} \frac{C_\alpha(\bar{x})}{\alpha!} D_x^\alpha \left(L_{\bar{x}}u(x)\right) \varrho^\alpha \\ &= L_{\bar{x}}u(x) + \sum_{1 \leqslant |\alpha| \leqslant m} \frac{C_\alpha(\bar{x})}{\alpha!} D_x^\alpha \left(L_{\bar{x}}u(x)\right) \varrho^\alpha \end{aligned} \tag{7}$$

where $C_0 = 1$, and $C_\alpha(\bar{x})$, $|\alpha| \leqslant m$, are given functions.

Intuitively, the new local approximation (7) can be viewed as a truncated Taylor series by taking $C_\alpha(x) = 1$, $\forall \alpha$. By substituting (3) into (7), the local approximation can explicitly be expressed as

$$\begin{aligned} u^{\ell}(x,\bar{x}) = {} & \mathbf{P}\left(\frac{x-\bar{x}}{\varrho}\right) \mathbf{M}^{-1}(\bar{x}) \int_{\Omega_y} \mathbf{P}^t \left(\frac{y-\bar{x}}{\varrho}\right) u(y) \phi_\varrho(y-\bar{x}) \, \mathrm{d}\Omega_y \\ & + \sum_{1 \leqslant |\alpha| \leqslant m} \frac{C_\alpha(\bar{x})\varrho^\alpha}{\alpha!} D_x^\alpha \left(\mathbf{P}\left(\frac{x-\bar{x}}{\varrho}\right)\right) \mathbf{M}^{-1}(\bar{x}) \int_{\Omega_y} \mathbf{P}^t \left(\frac{y-\bar{x}}{\varrho}\right) u(y) \phi_\varrho(y-\bar{x}) \, \mathrm{d}\Omega_y \end{aligned} \tag{8}$$

To globalize the approximation, we apply the moving procedure to (8),

$$Gu(x) := \lim_{\bar{x} \to x} u^{\ell}(x,\bar{x}) \tag{9}$$

which yields the following global approximation:

$$\begin{aligned} u(x) \approx Gu(x) = {} & \mathbf{P}^{(0)}(0)\mathbf{M}^{-1}(x) \int_{\Omega_y} \mathbf{P}^t \left(\frac{y-x}{\varrho}\right) u(y) \phi_\varrho(y-x) \, \mathrm{d}\Omega_y \\ & + C_1(x)\mathbf{P}^{(1)}(0)\mathbf{M}^{-1}(x) \int_{\Omega_y} \mathbf{P}^t \left(\frac{y-x}{\varrho}\right) u(y) \phi_\varrho(y-x) \, \mathrm{d}\Omega_y \\ & + \cdots \\ & + C_\mu(x)\mathbf{P}^{(\mu)}(0)\mathbf{M}^{-1}(x) \int_{\Omega_y} \mathbf{P}^t \left(\frac{y-x}{\varrho}\right) u(y) \phi_\varrho(y-x) \, \mathrm{d}\Omega_y \end{aligned} \tag{10}$$

where $\mathbf{P}^{(\alpha)}(0) := (1/\alpha!)D_x^{\alpha}\mathbf{P}(x/\varrho)\varrho^{\alpha}|_{x=0}$, $0 \leqslant |\alpha| \leqslant m$. $\mathbf{P}^{(\alpha)}(0)$ possesses particular simple structure,

$$\begin{aligned}
\mathbf{P}^{(0)}(0) &= (\underbrace{1,0,\ldots,0}_{\ell},\ldots,0)\\
\mathbf{P}^{(1)}(0) &= (0,\underbrace{1,0,\ldots}_{\ell-1},\ldots,0)\\
&\cdots\\
\mathbf{P}^{(\alpha)}(0) &= (0,\ldots,0,\underbrace{1,0,\ldots}_{\ell-i},0)\\
&\cdots\\
\mathbf{P}^{(\mu)}(0) &= (\underbrace{0,0,\ldots,0}_{\ell},1)
\end{aligned} \tag{11}$$

The generalized reproducing kernel representation is then expressed as

$$\begin{aligned}
\bar{\mathscr{R}}_{\varrho}^{m}u(x) = Gu(x) &= \sum_{|\alpha|\leqslant m} C_{\alpha}(x)\left\{\int_{\Omega}\mathbf{P}\left(\frac{y-x}{\varrho}\right)u(y)\phi_{\varrho}(y-x)\mathrm{d}\Omega_y\right\}\mathbf{b}^{(\alpha)}(x)\\
&= \sum_{|\alpha|\leqslant m} C_{\alpha}(x)\int_{\Omega}\mathscr{K}_{\varrho}^{[\alpha]}(y-x,x)u(y)\,\mathrm{d}\Omega_y
\end{aligned} \tag{12}$$

where $\mathscr{K}_{\varrho}^{[\alpha]}$ is the αth kernel,

$$\mathscr{K}_{\varrho}^{[\alpha]}(y-x,x) := \mathbf{P}\left(\frac{y-x}{\varrho}\right)\mathbf{b}^{(\alpha)}(x)\phi_{\varrho}(y-x) \quad \forall 0 \leqslant |\alpha| \leqslant m \tag{13}$$

and $\mathbf{b}^{(\alpha)}(x)$ is determined by algebraic equations

$$\mathbf{M}(x)\mathbf{b}^{(\alpha)}(x) = \{\mathbf{P}^{(\alpha)}(0)\}^{\mathrm{t}} \tag{14}$$

namely,

$$\mathbf{b}^{(\alpha)}(x) = \frac{1}{\Delta}\left\{(-1)^{1+i}A_{1i}(x),(-1)^{2+i}A_{2i}(x),\ldots,(-1)^{\ell+i}A_{\ell i}(x)\right\}^{\mathrm{t}} \tag{15}$$

where $\Delta = \det\mathbf{M}$ and A_{ij} are the minors of the global moment matrix $\mathbf{M}(x)$. Note that since the moment matrix $\mathbf{M}(x)$ is symmetric

$$\mathbf{P}^{(\alpha)}(0)\mathbf{M}^{-1}(x)\mathbf{P}^{\mathrm{t}}\left(\frac{y-x}{\varrho}\right) = \mathbf{P}\left(\frac{y-x}{\varrho}\right)\mathbf{M}^{-1}(x)\{\mathbf{P}^{(\alpha)}(0)\}^{\mathrm{t}}$$

If $C_{\alpha} = 0$, $\forall|\alpha| \neq 0$, (12) recovers the regular RKPM representation [10],

$$\mathscr{R}_{\varrho}^{m}u(x) = \int_{\Omega_y}\mathscr{K}_{\varrho}^{[0]}(y-x,x)u(y)\,\mathrm{d}\Omega_y \tag{16}$$

Equivalently, equation (14) can be interpreted as the following β-scale consistency conditions (see [10]):

$$\int_{\Omega}\left(\frac{y-x}{\varrho}\right)^{\beta}\mathscr{K}_{\varrho}^{[\alpha]}(y-x,x)\,\mathrm{d}\Omega_y = \delta_{\alpha\beta}, \quad 1 \leqslant |\beta| \leqslant m \tag{17}$$

When $\Omega = \mathbb{R}^n$ and $\varrho = 1$, $\mathbf{b}^{(\alpha)}(x) = \text{const.}$ and $\mathscr{K}_\varrho^{[\alpha]}(\cdot,\cdot) \equiv \mathscr{K}^{[\alpha]}(\cdot)$.[‡] Closely examining (17), one may find that

$$\int_{\mathbb{R}^n} \mathscr{K}^{[0]}(z)\,\mathrm{d}\Omega_z = 1 \quad \text{and} \quad \int_{\mathbb{R}^n} z^\beta \mathscr{K}^{[0]}(z)\,\mathrm{d}\Omega_z = 0, \quad 1 \leqslant |\beta| \leqslant m \tag{18}$$

Consequently, kernel $\mathscr{K}_\varrho^{[\alpha]}(x)$, $|\alpha| \neq 0$, satisfy $|\alpha| - 1$ order vanishing moment condition:

$$\int_{\mathbb{R}^n} z^\beta \mathscr{K}^{[\alpha]}(z)\,\mathrm{d}\Omega_z = 0, \quad 0 \leqslant |\beta| \leqslant |\alpha| - 1 \tag{19}$$

and some other vanishing moment conditions as well,

$$\int_{\mathbb{R}^n} z^\beta \mathscr{K}^{[\alpha]}(z)\,\mathrm{d}\Omega_z = 0, \quad |\beta + 1| \leqslant |\alpha| \leqslant m \tag{20}$$

If we restrict the window function $\phi \in H^{m+1}(\mathbb{R}) \cap C_0^m(\mathbb{R})$, the definition (13) will guarantee that at least[§] $\mathscr{K}^{[\alpha]}(x) \in L^2(\mathbb{R}) \cap L^1(\mathbb{R})$, and

$$\int_{\mathbb{R}} |x|^\beta |\mathscr{K}^{[\alpha]}(x)|\,\mathrm{d}x < +\infty, \quad \beta > 0 \tag{21}$$

which in turn, combining with (19), guarantees

$$C_{\mathscr{K}^{[\alpha]}} = (2\pi) \int_{\mathbb{R}_+} |\hat{\mathscr{K}}^{[\alpha]}(\zeta)|^2 \frac{\mathrm{d}\zeta}{\zeta} = (2\pi) \int_{\mathbb{R}_-} |\hat{\mathscr{K}}^{[\alpha]}(\zeta)|^2 \frac{\mathrm{d}\zeta}{|\zeta|} < +\infty \tag{22}$$

where $\hat{\mathscr{K}}^{[\alpha]}(\zeta)$ is the Fourier transform of $\mathscr{K}^{[\alpha]}(x)$,

$$\hat{\mathscr{K}}^{[\alpha]}(\zeta) := \frac{1}{\sqrt{2\pi}} \int_{-\infty}^{\infty} \exp(-\mathrm{i}\zeta z) \mathscr{K}^{[\alpha]}(z)\,\mathrm{d}z \tag{23}$$

Equation (22) is the admissible condition for the basis wavelet, or the mother wavelet (see [15] pp. 61–62; [16] pp. 7, 24–27; [19] p. 16; [20] pp. 5, 27; [21] pp. 61–72).[‖] The higher-dimensional extension of the admissible condition (22) is discussed in [16] pp. 33, 34.

In the following, we show that this is true in one-dimensional case (the extension to higher-dimensional cases can be readily followed). Since $\mathscr{K}^{[\alpha]}(x) \in C_0^m(\mathbb{R})$ for $m \geqslant 1$, it follows immediately that $\mathscr{K}^{[\alpha]}(x) \in L^1(\mathbb{R}) \cap L^2(\mathbb{R})$, and consequently, $\hat{\mathscr{K}}^{[\alpha]}$ is continuous, and $\hat{\mathscr{K}}^{[\alpha]} \in L^2(\mathbb{R})$. Furthermore, since $\mathscr{K}^{[\alpha]}(x) \in C_0^m(\mathbb{R})$, it is obvious that

$$\int_{-\infty}^{\infty} |x||\mathscr{K}^{[\alpha]}(x)|\,\mathrm{d}x < +\infty \tag{24}$$

[‡] This is also true when $\mathbf{x}$ is in the interior domain of a finite domain Ω

[§] The only exception in our numerical experiments is the Gaussian function; the associated kernel function, however, still satisfies this condition and (21)

[‖] The definition was first introduced by Grossmann and Morlet [18] in 1984

which implies that $\hat{\mathscr{K}}^{[\alpha]'}(\zeta) := \mathrm{d}\hat{\mathscr{K}}^{[\alpha]}/\mathrm{d}\zeta$ is also bounded. On the other hand, $\mathscr{K}^{[\alpha]}(x)$ is real,

$$\hat{\mathscr{K}}^{[\alpha]}(-\zeta) = \overline{\hat{\mathscr{K}}^{[\alpha]}}(\zeta) \Rightarrow |\hat{\mathscr{K}}^{[\alpha]}(-\zeta)|^2 \equiv |\hat{\mathscr{K}}^{[\alpha]}(\zeta)|^2 \tag{25}$$

Thus,

$$\int_{-\infty}^{\infty} \frac{|\hat{\mathscr{K}}^{[\alpha]}(\zeta)|^2}{|\zeta|}\,\mathrm{d}\zeta = 2\left\{\int_0^a \frac{|\hat{\mathscr{K}}^{[\alpha]}(\zeta)|^2}{\zeta}\,\mathrm{d}\zeta + \int_a^{+\infty} \frac{|\hat{\mathscr{K}}^{[\alpha]}(\zeta)|^2}{\zeta}\,\mathrm{d}\zeta\right\} \tag{26}$$

where $a<1$. Since $\hat{\mathscr{K}}^{[\alpha]}(\zeta) \in L^2(\mathbb{R})$ as shown early, $\exists C_1 > 0$ such that

$$\int_a^{+\infty} \frac{|\hat{\mathscr{K}}^{[\alpha]}(\zeta)|^2}{\zeta}\,\mathrm{d}\zeta < C_1 < +\infty \tag{27}$$

The remaining concern is the term, $\int_0^a |\hat{\mathscr{K}}^{[\alpha]}(\zeta)|^2/\zeta\,\mathrm{d}\zeta$. By the Cauchy inequality,

$$\int_0^a \frac{|\hat{\mathscr{K}}^{[\alpha]}(\zeta)|^2}{\zeta}\,\mathrm{d}\zeta \leqslant \sqrt{\int_0^a \left|\frac{\hat{\mathscr{K}}^{[\alpha]}(\zeta)}{\zeta}\right|^2 \mathrm{d}\zeta}\sqrt{\int_0^a |\hat{\mathscr{K}}^{[\alpha]}(\alpha)|^2\,\mathrm{d}\zeta} \tag{28}$$

From the vanishing moment conditions (19), one has

$$\int_{-\infty}^{\infty} \mathscr{K}^{[\alpha]}(x)\,\mathrm{d}x = 0 \Rightarrow \hat{\mathscr{K}}^{[\alpha]}(0) = 0 \tag{29}$$

By considering the facts that $\hat{\mathscr{K}}^{[\alpha]}(\zeta)$, and $\hat{\mathscr{K}}^{[\alpha]'}(\zeta)$ are continuous and bounded, there exists a constant, $C_2 > 0$, such that

$$\left|\frac{\hat{\mathscr{K}}^{[\alpha]}(\zeta)}{\zeta}\right| \leqslant \left|\frac{1}{\zeta}(\hat{\mathscr{K}}^{[\alpha]}(0) + \hat{\mathscr{K}}^{[\alpha]'}(\zeta^*)\zeta)\right| \leqslant |\hat{\mathscr{K}}^{[\alpha]'}(\zeta^*)| \leqslant C_2, \quad 0 < \zeta^* < a \tag{30}$$

Inequality (28) is then under control, which leads to the desired result¶

$$\int_{-\infty}^{0} \frac{|\hat{\mathscr{K}}^{[\alpha]}(\zeta)|^2}{|\zeta|}\,\mathrm{d}\zeta = \int_0^{\infty} \frac{|\hat{\mathscr{K}}^{[\alpha]}(\zeta)|^2}{\zeta}\,\mathrm{d}\zeta < +\infty \tag{31}$$

Thereby, coincidentally and legitimately, the higher scale kernels, $\mathscr{K}^{[\alpha]}(x), \alpha \neq 0$, are indeed a cluster of basic wavelet functions. It may be worthwhile noting that there is a strong resemblance in the construction procedure between this class of wavelets and '*the coiflets*', a particular wavelet, constructed by Daubechies [16, 22] and Beylkin *et al.* [23].

2.2. *Interpolation formulas*

To formulate a discrete interpolation scheme, a few definitions are in order. Let Λ be an index set of all particles. For a given bounded, simply connected region $\Omega \subset \mathbb{R}^n$, a particle distribution

¶ As shown in [16], condition $\int \mathrm{d}x\ \psi(x) = 0$ and $\int \mathrm{d}x(1+|x|)^\beta |\psi(x)| < \infty$ for some $\beta > 0$ which guarantee $|\hat{\psi}(\zeta)| \leqslant C|\zeta|^\alpha$, with $\alpha = \min(\beta, 1)$ and then the admissible condition (22)

$\mathscr{D}$ within Ω is defined as

$$\mathscr{D} := \{x_I \,|\, x_I \in \Omega, I \in \Lambda\} \tag{32}$$

For each $x_I \in \mathscr{D}$, there is an associated ball ω_I,

$$\omega_I := \{x \in \mathbb{R}^n \,|\, |x - x_I| \leqslant a_I \rho\} \tag{33}$$

where $a_I \sim \mathscr{O}(1)$ and ρ is defined as the *dilation parameter*. As defined in [10], for the admissible particle distribution, the dilation parameter is so chosen that it grants the following conditions:

1. For given constants $N_{\min}, N_{\max}$

$$N_{\min} \leqslant \text{card}\{\Lambda_I\} \leqslant N_{\max} \tag{34}$$

where Λ_I is a subset of Λ, i.e.

$$\Lambda_I := \{J \,|\, J \in \Lambda, \omega_J \cap \omega_I \neq \emptyset\} \tag{35}$$

2. The collection of all the balls,

$$\mathscr{F}_d := \{\omega_I \,|\, I \in \Lambda,\ x_I \in \mathscr{D},\ \text{and } \text{diam}(\omega_I) \leqslant a_I \rho\} \tag{36}$$

is a finite covering of domain Ω, i.e. $\bar{\Omega} \subset \bigcup_{I \in \Lambda} \omega_I$ we assume that there exists a constant C_d such that $\max_{I \in \Lambda}\{a_I\} \leqslant C_d$.

In what follows, we form the discrete interpolation formula by brutal discretization of the continuous integral representation, namely, equations (12), (13) and the moment equation (4), by Nyström quadrature method [24].

For given window function, $\phi > 0$, around particle x_I, the polynomial basis takes the value $\mathbf{P_I}(x) = \{P_{1I}, \ldots, P_{iI}, \ldots, P_{jI}, \ldots, P_{\ell I}\}$ with $P_{iI} = ((x_I - x)/\rho)^{\alpha}$ and $P_{jI} = ((x_I - x)/\rho)^{\beta}$, the discrete moment matrix (4) has the expression

$$\mathbf{M}^h(x) := \left\{M^h_{ij}(x)\right\}^{\ell \times \ell} = \left\{\sum_{I \in \Lambda} \left(\frac{x_I - x}{\rho}\right)^{\alpha+\beta} \phi_\rho(x_I - x) \Delta V_I\right\}^{\ell \times \ell} \tag{37}$$

Then, the αth-order discrete *correction function* is defined as

$$\mathscr{C}^{[\alpha]}_\rho(x_I - x, x) := \mathbf{P}^{(\alpha)}(0)\{\mathbf{M}^h(x)\}^{-1}\mathbf{P}^t\left(\frac{x_I - x}{\rho}\right) = \mathbf{P}\left(\frac{x_I - x}{\rho}\right)\mathbf{b}^{(\alpha)}(x) \tag{38}$$

Accordingly, the discrete αth scale kernel function is constructed as the modified window functions,

$$\mathscr{K}^{[\alpha]}_\varrho(x_I - x, x) := \mathscr{C}^{[\alpha]}_\rho(x_I - x, x)\phi_\rho(x_I - x) \tag{39}$$

Each kernel function generates a shape function sequence, i.e.

$$\{\Psi^{[\alpha]}_I(x)\}_{I \in \Lambda} := \left\{\alpha! \mathscr{K}^{[\alpha]}_\varrho(x_I - x, x)\Delta V_I\right\}_{I \in \Lambda} \tag{40}$$

The associated hierarchical interpolation is then set forth as

$$\mathscr{R}^{m[\alpha]}_{\rho,h} u(x) := \sum_{I=\Lambda} \Psi^{[\alpha]}_I(x) u(x_I) = \alpha! \sum_{I=\Lambda} \mathscr{K}^{[\alpha]}_\varrho(x_I - x, x) u(x_I) \Delta V_I \tag{41}$$

where $\{\Delta V_I\}_{I\in\Lambda}$ are the quadrature weights; they are so chosen such that

$$\Delta V_I \leqslant a_I^n \rho^n \quad \text{and} \quad \sum_{I\in\Lambda} \Delta V_I = \text{meas}(\Omega) \tag{42}$$

Equation (42) is often referred to as the stability condition [25, 10]. Note that in equation (38), the vector $\mathbf{b}^{(\alpha)}$ is determined by the discrete moment equations

$$\mathbf{M}^h(x)\mathbf{b}^{(\alpha)}(x) = \{\mathbf{P}^{(\alpha)}(0)\}^{\mathrm{t}} \tag{43}$$

One can readily verify that equation (43) is equivalent to the following discrete consistency condition:

$$\sum_{I\in\Lambda} \left(\frac{x_I - x}{\rho}\right)^{\beta} \mathscr{K}_{\varrho}^{[\alpha]}(x_I - x, x)\Delta V_I = \delta_{\alpha\beta} \tag{44}$$

2.3. Hierarchical partition of unity and hierarchical basis

From equation (44), one may find that the fundamental basis $\{\Psi_I^{(0)}(x)\}$ is a *signed partition of unity*, i.e.

$$\sum_{I\in\Lambda} \mathscr{K}_{\varrho}^{[0]}(x_I - x, x)\Delta V_I = \sum_{I\in\Lambda} \Psi_I^{[0]}(x) = 1 \tag{45}$$

which is the original moving least-squares reproducing kernel basis; whereas the higher order bases, $\{\Psi_I^{[\alpha]}(x)\}, \alpha \neq 0$, are the *partition of nullity*, so to speak, because by construction,

$$\sum_{I\in\Lambda} \Psi_I^{[\alpha]}(x) = \sum_{I\in\Lambda} \alpha! \mathscr{K}_{\varrho}^{[\alpha]}(x_I - x, x)\Delta V_I = 0, \quad 1 \leqslant |\alpha| \leqslant m \tag{46}$$

This is a very desirable property, because by inserting the higher-order basis into the fundamental basis, one will still have a partition of unity, i.e.

$$\begin{aligned} &\sum_{I\in\Lambda} (\mathscr{K}_{\varrho}^{[0]}(x_I - x, x) + 1!\mathscr{K}_{\varrho}^{[1]}(x_I - x, x) + \cdots + \alpha!\mathscr{K}_{\varrho}^{[\alpha]}(x_I - x, x))\Delta V_I \\ &\quad = \sum_{I\in\Lambda} \sum_{0 \leqslant |\beta| \leqslant |\alpha|} \Psi_I^{[\beta]}(x) = 1, \quad |\alpha| \leqslant m \end{aligned} \tag{47}$$

In the rest of the paper, we denote the mth-order hierarchical partition of unity on the particle distribution $\mathscr{D}$ as $\mathscr{H}_m := \{\{\Psi_I^{[\alpha]}(x)\}_{I\in\Lambda}\colon\ 0 \leqslant |\alpha| \leqslant m\}$. An example of such hierarchical partition of unity is displayed in Figure 1.

Since discrete wavelet functions form a partition of nullity, they are not linearly independent because in a partition of nullity there are extra, or redundant shape functions. Thus, the hierarchical partition of unity is at most a frame in global sense. Nevertheless, by careful selection, one can still form a hierarchical basis.

Definition 1 (*Hierarchical basis*). Choose $\mathring{\Lambda}_{[\alpha]} \subset\subset \Lambda,\ \forall 1 \leqslant |\alpha| \leqslant m$ and denote $n_{[\alpha]} := \text{card}\{\mathring{\Lambda}_{[\alpha]}\}$ such that $\forall f \in \text{span}\ \{\Psi_I^{[\alpha]}\}_{I\in\mathring{\Lambda}_{[\alpha]}}$, $\exists c_I$ and $c_I \not\equiv 0$,

$$f(x) = \sum_{I\in\mathring{\Lambda}_{[\alpha]}} c_I \Psi^{[\alpha]}(x)$$

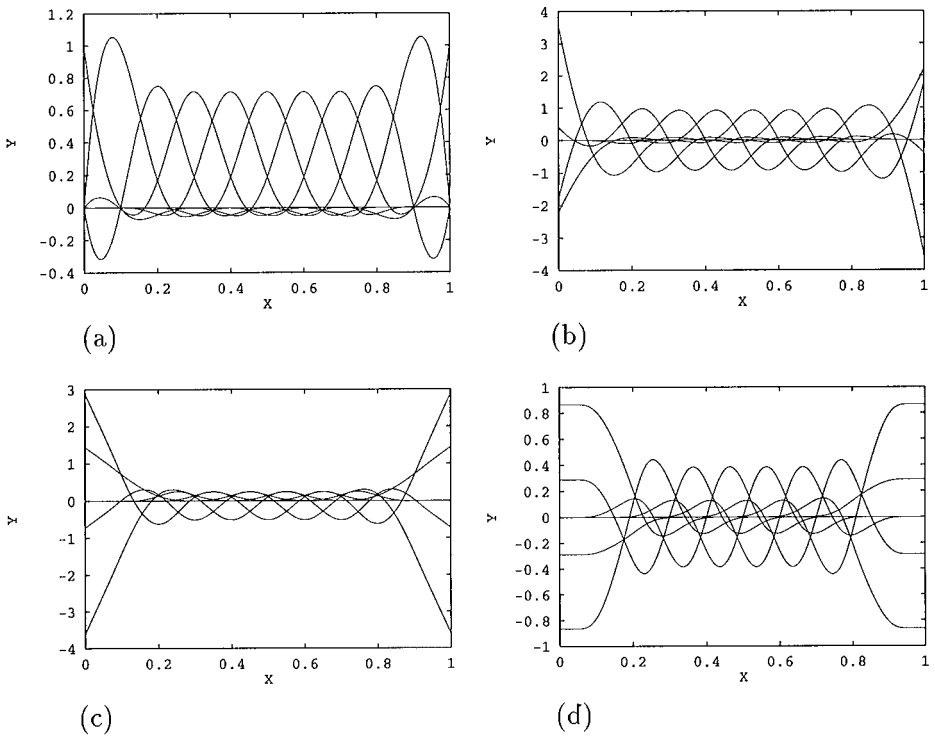

Figure 1. An example of hierarchical partition of unity: (a) $\{\mathscr{K}_\varrho^{[0]}(x_I - x,x)\}_{I\in\Lambda}$; (b) $\{\mathscr{K}_\varrho^{[1]}(x_I - x,x)\}_{I\in\Lambda}$; (c) $\{\mathscr{K}_\varrho^{[2]}(x_I - x,x)\}_{I\in\Lambda}$; (d) $\{\mathscr{K}_\varrho^{[3]}(x_I - x,x)\}_{I\in\Lambda}$

Define the global hierarchical basis

$$\{\Phi_j\}_{\Lambda_H} := \left\{\{\Psi_J^{[0]}\}_{J\in\Lambda}, \{\Psi_J^{[1]}\}_{J\in\mathring{\Lambda}_{[1]}}, \ldots, \{\Psi_J^{[\alpha]}\}_{J\in\mathring{\Lambda}_{[\alpha]}}\right\} \tag{48}$$

where $\Lambda_H := \{j \mid j = 1,\ldots,np, np+1,\ldots,n_H\}, n_H := (np + n_{[1]} + \cdots + n_{[\alpha]})$ and

$$\mathbf{A}_H := \{\alpha_{ij}\}^{n_H\times n_H}, \quad \alpha_{ij} = \int_\Omega \Phi_i\Phi_j \, \mathrm{d}\Omega$$

If $\det\{\mathbf{A}_H\} > 0$, we say $\{\Phi_i\}_{i\in\Lambda_H}$ is a hierarchical basis for the finite-dimensional space, $\mathscr{S}_H :=$ span $\left\{\{\Psi_I^{[0]}(x)\}_{I\in\Lambda}, \{\Psi_I^{[1]}(x)\}_{I\in\mathring{\Lambda}_{[1]}}, \ldots, \{\Psi_I^{[\alpha]}(x)\}_{I\in\mathring{\Lambda}_{[\alpha]}}\right\}$.

Remark 2.2. (1) By properly choosing the size of the compact support of the window function, one can form a wavelet-like basis by taking some shape functions out of the partition of nullity, usually the ones that are on the boundary. In this way, in the interior region, the hierarchical basis remains as a partition of unity. (2) In practice, by underintegration, it is possible that the stiffness matrix formed by hierarchical partition of unity is still invertible; in that case, however, spurious modes may occur. (3) By taking out certain number of extra shape functions from a partition of nullity, one may form an independent Group of basis functions from the partition of nullity, but it

does not automatically guarantee that (48) is an independent basis. In practice, exactly how many extra shape functions should be taken out is determined so far on a basis of trial and error.

Let $\mathbf{A}_H^{-1} := \{\beta_{ij}\}^{n_H \times n_H}$ and

$$\sum_l \alpha_{il}\beta_{lj} = \begin{cases} 1, & i = j \\ 0, & i \neq j \end{cases}$$

One can then define the dual basis

$$\{\tilde{\Phi}_i(x)\}_{i\in\Lambda_H}; \quad \tilde{\Phi}_i(x) := \sum_{i\in\Lambda_H} \beta_{ij}\Phi_j(x) \tag{49}$$

and subsequently the *reproducing kernel* of the hierarchical basis is

$$K_H(y,x) := \sum_{i,j\in\Lambda_H} \beta_{ij}\Phi_i(x)\Phi_j(y) \tag{50}$$

Thus, the generalized reproducing kernel formula becomes

$$\mathscr{R}_{\rho,h}^{m[H]} f(x) := \langle f(y), \quad K_H(y,x)\rangle_y = \sum_{i,j\in\Lambda_H} \beta_{ij}\left(\int_\Omega f(y)\Phi_j(y)\,\mathrm{d}\Omega_y\right)\Phi_i(x) \tag{51}$$

When $f \in \mathrm{span}\{\Phi_i(x)\}_{\Lambda_H}$, one can readily verify that $\mathscr{R}_{\rho,h}^{m[H]} f(x) = f(x)$.

3. EXAMPLES OF HIERARCHICAL PARTITION OF UNITY

In this section, several examples are given to illustrate how to construct a hierarchical partition of unity.

Example 3.1. In a 1-D segment $[-0{\cdot}5, 0{\cdot}5]$, let $m = 3$, $\ell = 3 + 1 = 4$. The hierarchical kernel functions are constructed in a *pointwise* fashion,

$$\mathscr{K}_\varrho^{[\alpha]}(x_I - x, x) := \mathbf{P}\left(\frac{x_I - x}{\varrho}\right)\mathbf{b}^{(\alpha)}(x)\phi_\varrho(x_I - x), \quad 0 \leqslant \alpha \leqslant 3 \tag{52}$$

The consistency conditions that the wavelet kernel packet satisfies are the following algebraic equation imposed on the vector $\mathbf{b}^{(\alpha)}(x)$:

$$\mathbf{M}^h(x)\mathbf{b}^{(\alpha)}(x) = \{\mathbf{P}^{(\alpha)}(0)\}^{\mathrm{t}}, \quad \alpha = 0, 1, 2, 3 \tag{53}$$

Or more explicitly,

$$\begin{pmatrix} m_0^h & m_1^h & m_2^h & m_3^h \\ m_1^h & m_2^h & m_3^h & m_4^h \\ m_2^h & m_3^h & m_4^h & m_5^h \\ m_3^h & m_4^h & m_5^h & m_6^h \end{pmatrix} \begin{pmatrix} b_1^{(\alpha)} \\ b_2^{(\alpha)} \\ b_3^{(\alpha)} \\ b_4^{(\alpha)} \end{pmatrix} = \begin{pmatrix} \delta_{\alpha 0} \\ \delta_{\alpha 1} \\ \delta_{\alpha 2} \\ \delta_{\alpha 3} \end{pmatrix} \tag{54}$$

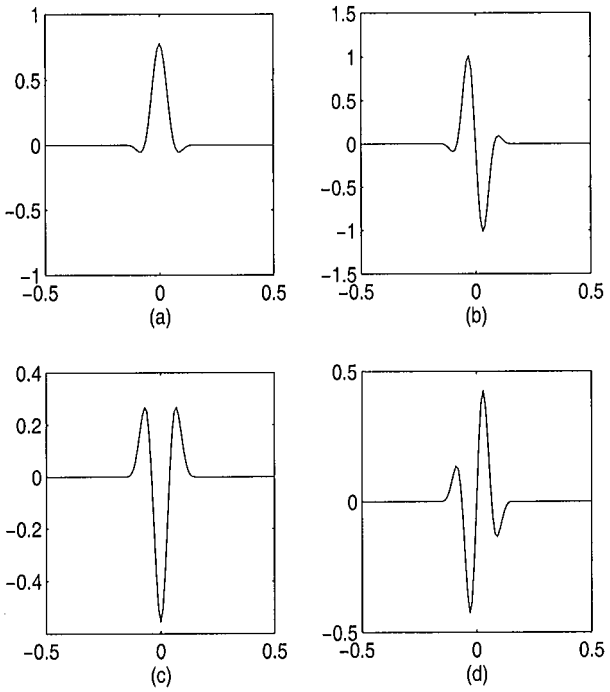

Figure 2. The hierarchical kernels at point $x_I = 0$ for $\mathbf{P} = (1, x, x^2, x^3)$: (a) fundamental kernel; (b) The first-order wavelet; (c) The second-order wavelet; (d) The third-order wavelet

where the αth discrete moment is defined as

$$m_\alpha^h(x) := \sum_{I=1}^{np} \left(\frac{x_I - x}{\varrho} \right)^\alpha \phi_\varrho(x_I - x) \Delta x_I. \tag{55}$$

In Figure 2, the constructed kernel function sequence is displayed at $x_I = 0$, and an uniform particle distribution (11 particles) is used in the computation. In computation, the parameter $\varrho = \Delta x$, and a fifth-order spline is used as window function ($a_I = 3{\cdot}3$). The second wavelet kernel in Figure 2(c) also resembles an upside-down Mexican hat.

Example 3.2. Let $\mathbf{P}(x) = (1, x_1, x_2)$. The discrete moment equations are

$$\begin{pmatrix} m_{00}^h & m_{10}^h & m_{01}^h \\ m_{10}^h & m_{20}^h & m_{11}^h \\ m_{01}^h & m_{11}^h & m_{02}^h \end{pmatrix} \begin{pmatrix} b_1^{(\alpha)} \\ b_2^{(\alpha)} \\ b_3^{(\alpha)} \end{pmatrix} = \begin{pmatrix} \delta_{\alpha(0,0)} \\ \delta_{\alpha(1,0)} \\ \delta_{\alpha(0,1)} \end{pmatrix} \tag{56}$$

One may note that here α is multiple index, i.e. $\alpha = (0,0), (1,0), (0,1)$. The hierarchical kernel functions are plotted in Figure 3.

Example 3.3. In this example, the dimension of the space is $n = 2$, $|\alpha| = m = 2$, and $\ell = 6$, and $\mathscr{K}_\varrho^{[\alpha]}(x_I - x, x) := \mathbf{P}((x_I - x)/\varrho)\mathbf{b}^{(\alpha)}(x)\phi_\varrho(x_I - x)$, with $x_I = (x_{1I}, x_{2I})$, $x = (x_1, x_2)$, and $\alpha = (0,0), (1,0)$,

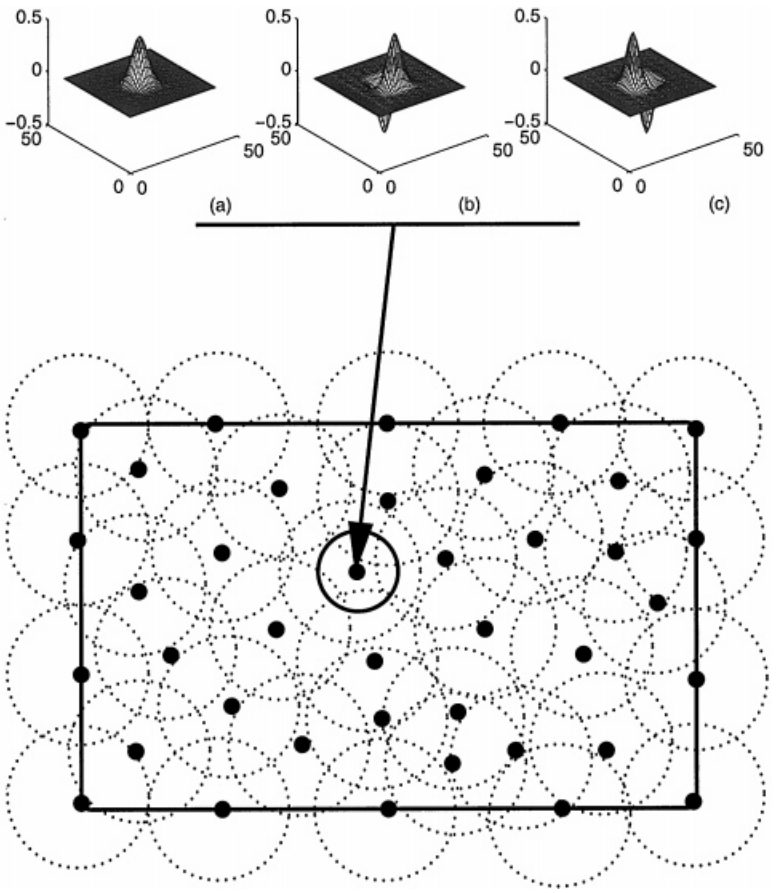

Figure 3. An illustration of 2-D hierarchical partition of unity with generating polynomial basis $\mathbf{P} = (1, x_1, x_2)$: (a) $\Psi_I^{[(0,0)]}(x)$; (b) $\Psi_I^{[(1,0)]}(x)$; (c) $\Psi_I^{[(0,1)]}(x)$

$(0,1),(2,0),(1,1),(0,2)$. The vector $\mathbf{b}^{(\alpha)}(x)$ is determined by the global moment equation that is similar to (54), namely,

$$\begin{pmatrix} m_{00}^h & m_{10}^h & m_{01}^h & m_{20}^h & m_{11}^h & m_{02}^h \\ m_{10}^h & m_{20}^h & m_{11}^h & m_{30}^h & m_{21}^h & m_{12}^h \\ m_{01}^h & m_{11}^h & m_{02}^h & m_{21}^h & m_{12}^h & m_{03}^h \\ m_{20}^h & m_{30}^h & m_{21}^h & m_{40}^h & m_{21}^h & m_{22}^h \\ m_{11}^h & m_{21}^h & m_{12}^h & m_{31}^h & m_{22}^h & m_{13}^h \\ m_{02}^h & m_{12}^h & m_{03}^h & m_{22}^h & m_{13}^h & m_{04}^h \end{pmatrix} \begin{pmatrix} b_1^{(\alpha)} \\ b_2^{(\alpha)} \\ b_3^{(\alpha)} \\ b_4^{(\alpha)} \\ b_5^{(\alpha)} \\ b_6^{(\alpha)} \end{pmatrix} = \begin{pmatrix} \delta_{\alpha(0,0)} \\ \delta_{\alpha(1,0)} \\ \delta_{\alpha(0,1)} \\ \delta_{\alpha(2,0)} \\ \delta_{\alpha(1,1)} \\ \delta_{\alpha(0,2)} \end{pmatrix} \tag{57}$$

Again, the above moment matrix is a full matrix for arbitrary particle distributions. By using a 2-D cubic spline as the window function, numerical computations have been carried out in a 2-D

domain $[-1,1]\times[-1,1]$ on an uniform 21×21 particle distribution. In Figure 4, the sequence of hierarchical kernel functions are displayed with respect to $x_I=(0,0)$. In the computation, the dilation vector $\varrho=(\varrho_1,\varrho_2)$ is chosen as $\varrho=(\Delta x,\Delta y)$ and $\Delta x=\Delta y=h$. The window function is a direct product of two cubic spline functions.

4. APPROXIMATION THEORY FOR THE HIERARCHICAL PARTITION OF UNITY

4.1. The differential consistency conditions

An intrinsic property of the above meshless hierarchical partition of unity is the following differential consistency conditions.

Lemma 4.1. *For the m-order polynomial based hierarchical partition of unity, the βth kernel function* $\mathscr{K}_\varrho^{[\beta]}$ *satisfies the following differential consistency conditions*:

$$\sum_{I\in\Lambda}\left(\frac{x_I-x}{\rho}\right)^\alpha D^\gamma_{x/\rho}\mathscr{K}_\varrho^{[\beta]}(x_I-x,x)\Delta V_I=\frac{\alpha!}{\beta!}\delta_{\alpha(\beta+\gamma)},\quad |\alpha|,|\beta|,|\gamma|\leqslant m \tag{58}$$

Proof: The proof is by induction on γ. First, assume $|\gamma|=0$ and then by (44)

$$\sum_{I\in\Lambda}\left(\frac{x_I-x}{\rho}\right)^\alpha D^\gamma_{x/\rho}\mathscr{K}_\varrho^{[\beta]}(x_I-x,x)\Delta V_I=\sum_{I\in\Lambda}\left(\frac{x_I-x}{\rho}\right)^\alpha \mathscr{K}_\varrho^{[\beta]}(x_I-x,x)\Delta V_I=\delta_{\alpha\beta} \tag{59}$$

Equation (58) holds.

Second, assume that (58) holds for $0\leqslant|\gamma|\leqslant m-1$, namely,

$$\sum_{I\in\Lambda}\left(\frac{x_I-x}{\rho}\right)^\alpha D^\gamma_{x/\rho}\mathscr{K}_\varrho^{[\beta]}(y-x,x)\Delta V_I=\frac{\alpha!}{(\alpha-\gamma)!}\delta_{\alpha(\beta+\gamma)} \tag{60}$$

We need to show that (58) holds for $0\leqslant|\gamma'|\leqslant m$. Let $\gamma'=\gamma+\eta,\eta=(\eta_1,\eta_2,\ldots,\eta_n),|\eta|=1,0\leqslant|\gamma'|\leqslant m$. Since $|\eta|=1$, differentiate (60) and then by the chain rule,

$$\sum_{I\in\Lambda}\left\{D^\eta_x\left(\frac{x_I-x}{\rho}\right)^\alpha D^\gamma_{x/\rho}\mathscr{K}_\varrho^{[\beta]}(x_I-x,x)+\left(\frac{x_I-x}{\rho}\right)^\alpha \rho^{-\eta}D^{\gamma+\eta}_{x/\rho}\mathscr{K}_\varrho^{[\beta]}(x_I-x,x)\right\}\Delta V_I=0 \tag{61}$$

It can be shown that

$$\begin{aligned}D^\eta_x\left(\frac{x_I-x}{\rho}\right)^\alpha &=(-1)^{|\eta_1|+|\eta_2|+\cdots+|\eta_n|}\frac{\alpha_1!\alpha_2!\cdots\alpha_n!\cdot\rho^{-\eta_1-\eta_2-\cdots-\eta_n}}{(\alpha_1-\eta_1)!(\alpha_2-\eta_2)!\cdots(\alpha_n-\eta_n)!}\\ &\quad\times\left(\frac{x_{1I}-x_1}{\rho}\right)^{\alpha_1-\eta_1}\left(\frac{x_{2I}-x_2}{\rho}\right)^{\alpha_2-\eta_2}\cdots\left(\frac{x_{nI}-x_n}{\rho}\right)^{\alpha_n-\eta_n}\\ &=(-1)^{|\eta|}\frac{\rho^{-\eta}\alpha!}{(\alpha-\eta)!}\left(\frac{x_I-x}{\rho}\right)^{\alpha-\eta}\end{aligned} \tag{62}$$

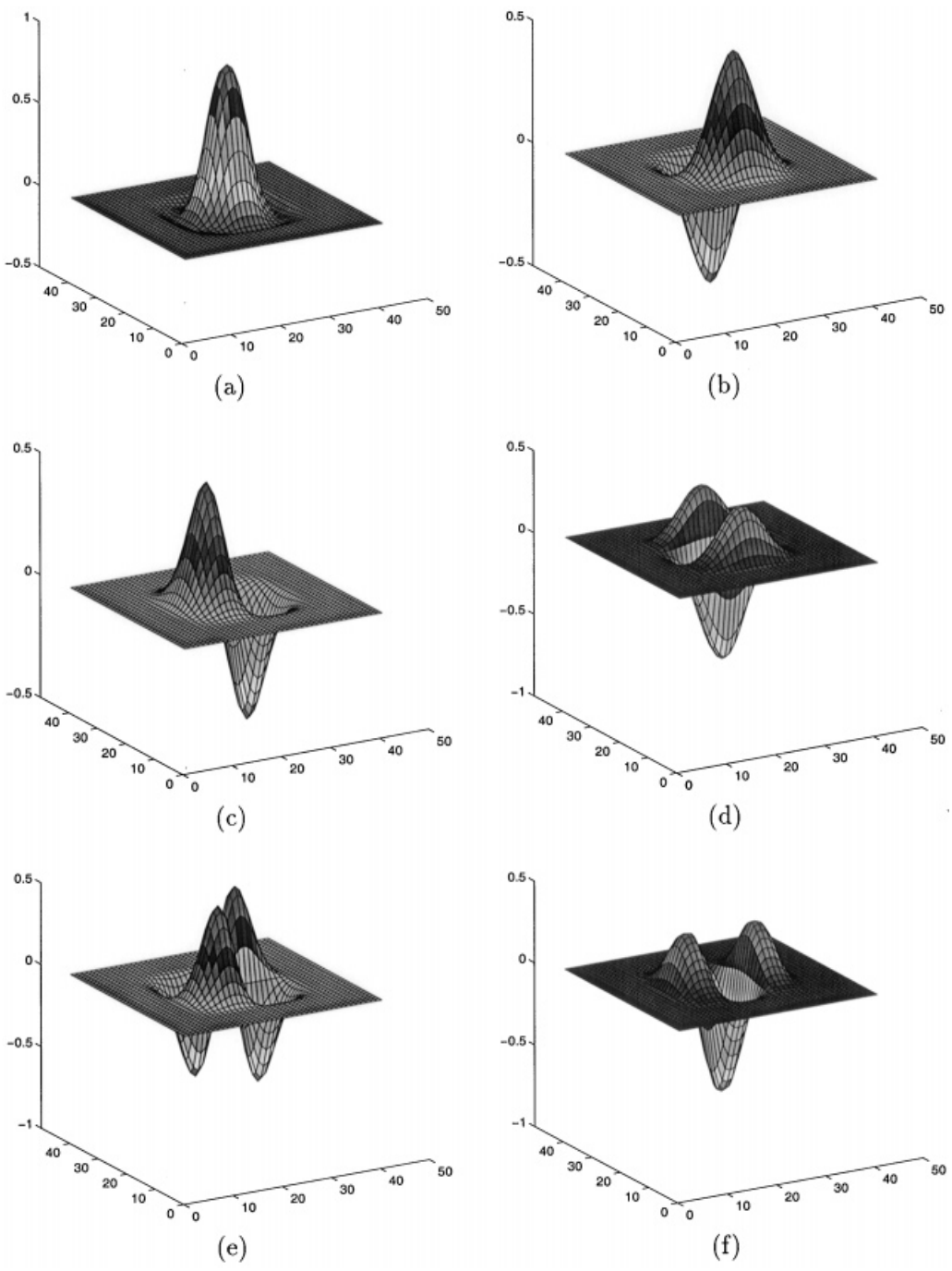

Figure 4. A 2-D hierarchical kernel sequence: (a) $\Psi_I^{[0,0]}(x)$; (b) $\Psi_I^{[1,0]}(x)$; (c) $\Psi_I^{[0,1]}(x)$; (d)$\Psi_I^{[2,0]}(x)$; (e) $\Psi_I^{[1,1]}(x)$; (f) $\Psi_I^{[0,2]}(x)$

Table I. Differential consistency conditions for $\mathscr{K}_\varrho^{[0]}$

$M_3^{[0]}=0$	$M_3^{[0](1)}=0$	$M_3^{[0](2)}=0$	$M_3^{[0](3)}=3!$
$M_2^{[0]}=0$	$M_2^{[0](1)}=0$	$M_2^{[0](2)}=2!$	$M_2^{[0](3)}=0$
$M_1^{[0]}=0$	$M_1^{[0](1)}=1!$	$M_1^{[0](2)}=0$	$M_1^{[0](3)}=0$
$M_0^{[0]}=0!$	$M_0^{[0](1)}=0$	$M_0^{[0](2)}=0$	$M_0^{[0](3)}=0$

Thereby, equation (61) yields

$$\begin{aligned}
&\sum_{I\in\Lambda}\left(\frac{x_I-x}{\rho}\right)^\alpha D^{\gamma'}_{x/\rho}\mathscr{K}_\varrho^{[\beta]}(x_I-x,x)\Delta V_I\\
&\quad=\frac{(-1)^{|\eta|+1}\alpha!}{(\alpha-\eta)!}\sum_{I\in\Lambda}\left(\frac{x_I-x}{\rho}\right)^{\alpha-\eta} D^{\gamma}_{x/\rho}\mathscr{K}_\varrho^{[\beta]}(x_I-x,x)\Delta V_I\\
&\quad=\frac{\alpha!}{(\alpha-\eta)!}\frac{(\alpha-\eta)!}{(\alpha-\eta-\gamma)!}\delta_{(\alpha-\eta)(\beta+\gamma)}=\frac{\alpha!}{(\alpha-\gamma')!}\delta_{(\alpha-\eta)(\beta+\gamma)}=\frac{\alpha!}{\beta!}\delta_{\alpha(\beta+\gamma')}
\end{aligned}\tag{63}$$

In the second step, (60) is used, and in the last step, the identity, $\delta_{(\alpha-\eta)(\beta+\gamma)}=\delta_{\alpha(\beta+\gamma')}$, is used. □

Let

$$M_\alpha^{[\beta]}:=\sum_{I\in\Lambda}\left(\frac{x_I-x}{\varrho}\right)^\alpha \mathscr{K}_\varrho^{[\beta]}(x_I-x,x)\Delta V_I \tag{64}$$

$$M_\alpha^{[\beta](\gamma)}:=\sum_{I\in\Lambda}\left(\frac{x_I-x}{\varrho}\right)^\alpha D^{\gamma}_{x/\varrho}\mathscr{K}_\varrho^{[\beta]}(x_I-x,x)\Delta V_I \tag{65}$$

The differential consistency conditions for the fundamental kernel and the wavelet kernels can be interpreted as the following moment identities:

$$M_\alpha^{[0](\gamma)}=\alpha!\delta_{\alpha\gamma},\quad M_\alpha^{[\beta](\gamma)}=\frac{\alpha!}{\beta!}\delta_{\alpha(\beta+\gamma)} \tag{66}$$

Tables I–IV display graphically the differential consistency conditions of the hierarchical partition of unity in Example 3.1. For the fundamental kernel, all the non-zero entries lie on the main diagonal line of the table; for the first-order wavelet kernel, all the non-zero entries lie on the first sub-diagonal line; and for the second-order wavelet, the non-zero entries move to the second sub-diagonal line, and the pattern continues untill the third-order wavelet.

4.2. Interpolation estimate

The main result of this section is the following interpolation estimate for the βth-order kernel interpolant.

Table II. Differential consistency conditions for the first wavelet $\mathscr{K}_\varrho^{[1]}$

$M_3^{[1]}=0$	$M_3^{[1](1)}=0$	$M_3^{[1](2)}=3!$	$M_3^{[1](3)}=0$
$M_2^{[1]}=0$	$M_2^{[1](1)}=2!$	$M_2^{[1](2)}=0$	$M_2^{[1](3)}=0$
$M_1^{[1]}=1$	$M_1^{[1](1)}=0$	$M_1^{[1](2)}=0$	$M_1^{[1](3)}=0$
$M_0^{[1]}=0$	$M_0^{[1](1)}=0$	$M_0^{[1](2)}=0$	$M_0^{[1](3)}=0$

Table III. Differential consistency conditions for the second wavelet $\mathscr{K}_\varrho^{[2]}$

$M_3^{[2]}=0$	$M_3^{[2](1)}=3!/2!$	$M_3^{[2](2)}=0$	$M_3^{[2](3)}=0$
$M_2^{[2]}=1$	$M_2^{[2](1)}=0$	$M_2^{[2](2)}=0$	$M_2^{[2](3)}=0$
$M_1^{[2]}=0$	$M_1^{[2](1)}=0$	$M_1^{[2](2)}=0$	$M_1^{[2](3)}=0$
$M_0^{[2]}=0$	$M_0^{[2](1)}=0$	$M_0^{[2](2)}=0$	$M_0^{[2](3)}=0$

Table IV. Differential consistency conditions for the third wavelet $\mathscr{K}_\varrho^{[3]}$

$M_3^{[3]}=1$	$M_3^{[3](1)}=0$	$M_3^{[3](2)}=0$	$M_3^{[3](3)}=0$
$M_2^{[3]}=0$	$M_2^{[3](1)}=0$	$M_2^{[3](2)}=0$	$M_2^{[3](3)}=0$
$M_1^{[3]}=0$	$M_1^{[3](1)}=0$	$M_1^{[3](2)}=0$	$M_1^{[3](3)}=0$
$M_0^{[3]}=0$	$M_0^{[3](1)}=0$	$M_0^{[3](2)}=0$	$M_0^{[3](3)}=0$

Theorem 4.1 (Local estimate). *Assume* $u\in H^{m+1}(\Omega)\cap C^0(\Omega)$ *and* $\phi\in C_0^m(\Omega)\cap H^{m+1}(\Omega)$** *and* $2m\geqslant n$, *where* n *is the dimension of the space. For given bounded domain* Ω, *there is a meshless hierarchical discretization* $\{\mathscr{D},\mathscr{F}_\rho,\mathscr{H}_m\}$. *Then* $\forall\omega_I\in\mathscr{F}_\rho$ *and* $\mathscr{R}_{\varrho,h}^{m[\beta]}u\in\operatorname{span}\{\mathscr{H}_m\}$ *the following interpolation error estimate holds*:

$$\|\rho^\beta D_x^\beta u(x)-\mathscr{R}_{\varrho,h}^{m[\beta]}u(x)\|_{H^\gamma(\omega_I\cap\Omega)}\leqslant, C_I\varrho^{m+1-|\gamma|}\|u\|_{H^{m+1}(\omega_I\cap\Omega)},\quad \forall 0\leqslant|\beta|,|\gamma|,|\beta+\gamma|\leqslant m \tag{67}$$

where $\mathscr{R}_{\varrho,h}^{m[\beta]}u(x)$ is given in equation (41).

Proof. We only need to show that $\exists C$ such that for fixed $I\in\Lambda$,

$$|D_x^\gamma((\rho^\beta D_x^\beta u(x)-\mathscr{R}_{\varrho,h}^{m[\beta]}u(x))|_{L^2(\omega_I\cap\Omega)}\leqslant C\varrho^{m+1-|\gamma|}|u|_{H^{m+1}(\omega_I\cap\Omega)},\quad \forall 0\leqslant|\beta|,|\gamma|,|\beta+\gamma|\leqslant m \tag{68}$$

** This restriction is imposed for the sake of an easy proof; it may be relaxed

By Taylor's expansion, for $x \in \omega_I \cap \Omega$, one has

$$
\begin{aligned}
D_x^\gamma \left(\rho^\beta D_x^\beta u - \mathscr{R}_{\varrho,h}^{m[\beta]} u \right) &= \rho^\beta D_x^{\beta+\gamma} u(x) - \beta! D_x^\gamma \left[\sum_{J \in \Lambda_I} \mathscr{K}_\varrho^{[\beta]}(x_J - x, x) u(x_J) \Delta V_J \right] \\
&= \rho^\beta D_x^{\beta+\gamma} u(x) - \beta! \sum_{J \in \Lambda_I} \left(D_x^\gamma \mathscr{K}_\varrho^{[\beta]}(x_J - x, x) \right) \\
&\quad \times \left(\sum_{|\alpha| < m+1} \frac{1}{\alpha!} (x_J - x)^\alpha D^\alpha u(x) + \sum_{|\alpha| = m+1} \left(\frac{m+1}{\alpha!} \right) (x_J - x)^\alpha \right. \\
&\quad \left. \times \left(\int_0^1 s^m D^\alpha u(x_J + s(x - x_J)) \, \mathrm{d}s \right) \right) \Delta V_J
\end{aligned} \tag{69}
$$

Applying the differential consistency condition (58)–(69), one may find that

$$
\begin{aligned}
\left| D_x^\gamma \left(\rho^\beta D_x^\beta u - \mathscr{R}_{\varrho,h}^{m[\beta]} u \right) \right| &= \left| \rho^\beta D_x^{\beta+\gamma} u(x) - \rho^\beta D_x^{\beta+\gamma} u(x) \right. \\
&\quad - \beta! \sum_{J \in \Lambda_I} \sum_{|\alpha| = m+1} \left(\frac{m+1}{\alpha!} \right) (x_J - x)^\alpha D_x^\gamma \mathscr{K}_\varrho^{[\beta]}(x_J - x, x) \\
&\quad \left. \times \left(\int_0^1 s^m D^\alpha u(x_J + s(x - x_J)) \, \mathrm{d}s \right) \Delta V_J \right| \\
&\leqslant C(\beta, m) \left| \sum_{J \in \Lambda_I} \sum_{|\alpha| = m+1} \frac{(x_J - x)^\alpha}{\alpha!} D_x^\gamma \mathscr{K}_\varrho^{[\beta]}(x_J - x, x) \right. \\
&\quad \left. \times \left(\int_0^1 s^m D^\alpha u(x_J + s(x - x_J)) \, \mathrm{d}s \right) \Delta V_J \right|
\end{aligned} \tag{70}
$$

Let $\zeta = x/\rho$, $\zeta_J = x_J/\rho$ and $E_{\omega_I}^{\gamma,m}(x) := |D_x^\gamma(\rho^\beta D^\beta u - \mathscr{R}_{\varrho,h}^{m[\beta]} u)|$. Considering the fact that $\mathscr{K}^{[\beta]}(\zeta_J - \zeta, \zeta)$ is compact supported and its support size equals $\mathrm{diam}\{\omega_J\}$, then identically,

$$
\mathscr{K}^{[\beta]}(\zeta_J - \zeta, \zeta) = \mathscr{K}^{[\beta]}(\zeta_J - \zeta, \zeta) \chi(\zeta_J - \zeta)
$$

where $\chi(\zeta_J - \zeta)$ is the characteristic function of ω_J, i.e.

$$
\chi(\zeta_J - \zeta) = \begin{cases} 1, & |\zeta_J - \zeta| \leqslant a_J \\ 0, & |\zeta_J - \zeta| > a_J \end{cases}
$$

Repeat using the Cauchy–Schwarz inequality yields

$$
\begin{aligned}
E_{\omega_I}^{\gamma,m}(x) \leqslant C(\beta, m) \rho^{m+1-|\gamma|-n} &\left| \sum_{J \in \Lambda_I} \sum_{|\alpha| = m+1} \frac{(\zeta_J - \zeta)^\alpha}{\alpha!} (D_\zeta^\gamma \mathscr{K}^{[\beta]}(\zeta_J - \zeta, \zeta)) \right. \\
&\left. \times \left(\int_0^1 s^m D^\alpha u(\rho[\zeta_J + s(\zeta - \zeta_J)]) \, \mathrm{d}s \right) \chi(\zeta_J - \zeta) \Delta V_J \right|
\end{aligned}
$$

$$\leqslant C(\beta,m)\rho^{m+1-|\gamma|-n}\left|\int_0^1 \sum_{J\in\Lambda_I}\left\{\left[\sum_{|\alpha|=m+1}\left(\frac{(\zeta_J-\zeta)^\alpha}{\alpha!}D_\zeta^\gamma \mathscr{K}^{[\beta]}(\zeta_J-\zeta,\zeta)\right)^2\right]^{1/2}\right.$$
$$\left.\times\left[\sum_{|\alpha|=m+1}(s^m D^\alpha u(\rho[\zeta_J+s(\zeta-\zeta_J)]))^2\right]^{1/2}\right\}\chi(\zeta_J-\zeta)\Delta V_J\,\mathrm{d}s\Bigg|$$
$$\leqslant C(\beta,m)\rho^{m+1-|\gamma|-n}\left|\int_0^1\left\{\left[\sum_{J\in\Lambda_I}\chi(\zeta_J-\zeta)\Delta V_J\right.\right.\right.$$
$$\times\sum_{|\alpha|=m+1}\left(\frac{(\zeta_J-\zeta)^\alpha}{\alpha!}D_\zeta^\gamma \mathscr{K}^{[\beta]}(\zeta_J-\zeta,\zeta)\right)^2\Bigg]^{1/2}\left[\sum_{J\in\Lambda_I}\chi(\zeta_J-\zeta)\Delta V_J\right.$$
$$\left.\left.\left.\times\sum_{|\alpha|=m+1}(s^m D^\alpha u(\rho[\zeta_J+s(\zeta-\zeta_J)]))^2\right]^{1/2}\right\}\mathrm{d}s\right| \tag{71}$$

Since $D_\zeta^\gamma \mathscr{K}^{[\beta]}(\zeta_J-\zeta,\zeta)$ is bounded and $\chi(\zeta_J-\zeta)|\zeta_J-\zeta|\leqslant a_J\leqslant C_d$,

$$E_{\omega_I}^{\gamma,m}(x)\leqslant C(\alpha,\beta,\gamma,C_d,m)\rho^{m+1-|\gamma|-n}\left|\int_0^1\left[\sum_{J\in\Lambda_I}\Delta V_J\right]^{1/2}\cdot\left[\sum_{J\in\Lambda_I}\chi(\zeta_J-\zeta)\Delta V_J\right.\right.$$
$$\left.\left.\times\sum_{|\alpha|=m+1}(s^m D^\alpha u(\rho[\zeta_J+s(\zeta-\zeta_J)]))^2\right]^{1/2}\mathrm{d}s\right| \tag{72}$$

By invoking the stability condition, $\sum_{J\in\Lambda_I}\Delta V_J\leqslant N_{\max}C_d^n\rho^n$, it follows that

$$|\rho^\beta D_x^\beta u-\mathscr{R}_{\varrho,h}^{m[\beta]}u|_{H^{|\gamma|}(\omega_I\cap\Omega)}\leqslant C(\alpha,\beta,\gamma,C_d,m,N_{\max})\rho^{m+1-|\gamma|-n/2}$$
$$\times\left\{\sum_{J\in\Lambda_I}\int_0^1\int_{\omega_I\cap\omega_J\cap\Omega}\sum_{|\alpha|=m+1}s^{2m}(D^\alpha u(x_J+s(x-x_J)))^2\right.$$
$$\left.\times\mathrm{d}\Omega_x\,\mathrm{d}s\Delta V_J\right\}^{1/2}$$

Change variables $z=x_J+s(x-x_J)$, and $\Omega_x\,\mathrm{d}s=s^{-n}\mathrm{d}\Omega_z\,\mathrm{d}s$. The new integration domain for each $J\in\Lambda_I$ is

$$A_J(z,s)=\{(z,s)\,|\,s\in(0,1],\ \tilde{\omega}_I\cap\tilde{\omega}_J\cap\tilde{\Omega}\} \tag{73}$$

where $\forall J\in\Lambda_I$ and $\tilde{\omega}_J:=\{z|(1/s)|z-z_J|\leqslant a_J\rho,\ 0<s\leqslant 1\}$.

Since $s\leqslant 1$ and $z_J=x_J$, one has $\tilde{\omega}_J\subset\omega_J\ \forall J\in\Lambda_I$, and

$$|\rho^\beta D_x^\beta u-\mathscr{R}_{\varrho,h}^{m[\beta]}u|_{H^{|\gamma|}(\omega_I\cap\Omega)}\leqslant C(\alpha,\beta,\gamma,C_d,m,N_{\max})\rho^{m+1-|\gamma|-n/2}$$
$$\times\left\{\sum_{J\in\Lambda_I}\Delta V_J\int_0^1\int_{\omega_I\cap\omega_J\cap\Omega}\sum_{|\alpha|=m+1}s^{2m-n}(D^\alpha u(z))^2\,\mathrm{d}\Omega_z\,\mathrm{d}s\right\}^{1/2}$$

By the assumption $2m-n\geqslant 0$, the Fubini's theorem, and the stability condition,

$$|\rho^{\beta}D_x^{\beta}u-\mathscr{R}_{\varrho,h}^{m[\beta]}u|_{H^{|\gamma|}(\omega_I\cap\Omega)}\leqslant C(\alpha,\beta,\gamma,C_d,m,n,N_{\max})\rho^{m+1-|\gamma|}|u|_{H^{m+1}(\omega_I\cap\Omega)} \tag{74}$$

□

Note that the fact that the constant C in Equation (74) is a function of C_d implies that C does not depend on a_I.

Theorem 4.2 (Global estimate). *For* $u\in H^{m+1}(\Omega)\cap C^0(\Omega)$, $\phi\in C_0^m(\Omega)\cap H^{m+1}(\Omega)$, *the global discretization*, $\{\mathscr{D},\mathscr{F}_\rho,\mathscr{H}_m\}$, *yields the following estimate*:

$$\|\rho^{\beta}D_x^{\beta}u-\mathscr{R}_{\varrho,h}^{m[\beta]}u\|_{H^{|\gamma|}(\Omega)}\leqslant C\rho^{m+1-|\gamma|}\|u\|_{H^{m+1}(\Omega)},\quad 0\leqslant|\beta|\leqslant m \tag{75}$$

Proof. Again, we only need to show following semi-norm estimate

$$|\rho^{\beta}D_x^{\beta}u-\mathscr{R}_{\varrho,h}^{m[\beta]}u|_{H^{|\gamma|}(\Omega)}\leqslant C\rho^{m+1-|\gamma|}|u|_{H^{m+1}(\Omega)} \tag{76}$$

By (74) $\exists 0<C_0<\infty$ such that

$$\begin{aligned}|\rho^{\beta}D_x^{\beta}u-\mathscr{R}_{\varrho,h}^{m[\beta]}u|_{H^{|\gamma|}(\Omega)}^2&\leqslant\sum_{I\in\Lambda}|\rho^{\beta}D_x^{\beta}u-\mathscr{R}_{\varrho,h}^{m[\beta]}u|_{H^{|\gamma|}(\omega_I\cap\Omega)}^2\\&\leqslant C_0^2\rho^{2(m+1-|\gamma|)}\sum_{I\in\Lambda}|u|_{H^{m+1}(\omega_I\cap\Omega)}^2\end{aligned} \tag{77}$$

where C_0 can be chosen as the constant C in (74).

The key technical ingredient of the global estimate is the following fact: there exists an auxiliary, virtual background cell discretization, $\{\mathring{\omega}_I\}_{I\in\Lambda}$, that has the properties:

$$x_I\in\mathring{\omega}_I\cap\Omega \tag{78}$$

$$\mathring{\omega}_I\subset\omega_I \tag{79}$$

$$\bigcup_{I\in\Lambda}\mathring{\omega}_I\cap\Omega=\Omega \tag{80}$$

in which

$$\operatorname{int}\{\mathring{\omega}_I\}\cap\operatorname{int}\{\mathring{\omega}_J\}=\begin{cases}\operatorname{int}\{\mathring{\omega}_I\}, & I=J\\ \emptyset, & I\neq J\end{cases} \tag{81}$$

such that $\forall I\in\Lambda$

$$\omega_I\cap\Omega\subset\bigcup_{J\in\Lambda_I}\mathring{\omega}_J\cap\Omega \tag{82}$$

We show that the claim is true by contradictory argument.

Suppose there is no such virtual cell discretization (78)–(81) that satisfies the condition (82). Then, $\exists I\in\Lambda$ and $x\in\Omega$ such that

$$x\in\omega_I\cap\Omega\quad\text{but } x\notin\bigcup_{J\in\Lambda_I}\mathring{\omega}_J\cap\Omega$$

It is obvious that $x\notin\bigcup_{J\in\Lambda\setminus\Lambda_I}\mathring{\omega}_J\cap\Omega$, which leads to the contradiction $x\notin\Omega$ because of condition (80).

Hence, the overlapping condition (34) suggests that

$$\sum_{I\in\Lambda}|u|^2_{H^{m+1}(\omega_I\cap\Omega)} \leqslant \sum_{I\in\Lambda}\sum_{J\in\Lambda_I}|u|^2_{H^{m+1}(\hat{\omega}_I\cap\Omega)} \leqslant N_{\max}\sum_{I\in\Lambda}|u|^2_{H^{m+1}(\hat{\omega}_I\cap\Omega)} = N_{\max}|u|^2_{H^{m+1}(\Omega)} \tag{83}$$

Estimate (76) follows immediately, and consequently, (75).

Remark 4.1. (1) When $\beta=0$, the estimate (75) recovers the error estimate for the regular reproducing kernel interpolant [10]. (2) By taking advantage of the global differential consistency conditions, there is no need to use the notion of 'affine equivalence' in the proof, which is a major difference between the current proof and the finite element type proofs. (3) Because the βth wavelet kernel satisfies $|\beta|-1$ order vanishing moment conditions, Theorem 4.2 indicates that its sampling range is up to $\rho^{|\beta|}$ scale in the physical space. Apparently, the larger the absolute value $|\beta|$, the finer scale the wavelet kernel can represent, which, in other words, implies that each wavelet kernel has a different bandwidth in the frequency domain.†† In this sense, the hierarchical partition of unity is a wavelet kernel packet, because we are basically dealing with a special type of least-square filters. It is noteworthy pointing out the similarity between the wavelet based hierarchical partition of unity and the wavelet packet invented by Coifman and Meyer [12].

4.3. Synchronized reproducing kernel interpolants

Using hierarchical kernels, one also can construct a so-called synchronized reproducing kernel interpolant via a combination of different kernels. In Section 2, we define the generalized reproducing kernel by the following expansion:

$$\mathscr{K}^{[s]}_{\varrho}(\cdot,\cdot) := \sum_{|\alpha|\leqslant m} C_\alpha \mathscr{K}^{[\alpha]}_{\varrho}(\cdot,\cdot) \tag{84}$$

And the so-called synchronized reproducing kernel interpolant is referred to as the following sampling, or filtering procedure,

$$\mathscr{R}^{m[s]}_{\varrho,h}u(x) := \sum_{I\in\Lambda}\mathscr{K}^{[s]}_{\varrho}(x_I-x,x)u(x_I)\Delta V_I \tag{85}$$

Theorem 4.3 (Synchronized convergence). *Assume* $u\in[tH^{m+1}(\Omega)\cap C^0(\Omega)$ *and* $\phi\in C^m_0(\Omega)\cap H^{m+1}(\Omega)$. *By fixing* p, $0\leqslant p\leqslant m$, *and choosing* $C_0=1$, $C_\beta=\beta!$, $|\beta|=p$, *and* $C_\alpha=0$, $\alpha\neq 0,\beta$, *then following interpolation error estimate holds for the m-order synchronized kernel interpolant*,

$$\|u(x)-\mathscr{R}^{m[s]}_{\varrho,h}u(x)\|_{H^{|\gamma|}(\Omega)} \leqslant C_\gamma\rho^p\|u\|_{H^{m+1}(\Omega)}, \quad 0\leqslant|\gamma|\leqslant m+1-p \tag{86}$$

where $\mathscr{R}^{m[s]}_{\varrho,h}u(x)$ *is defined in equation* (85).

Proof. By Theorem 4.2, for fixed index γ, $0\leqslant|\gamma|\leqslant m$,

$$\|u-\mathscr{R}^{m[s]}_{\varrho,h}u\|_{H^{|\gamma|}(\Omega)} = \|u-\mathscr{R}^{m[0]}_{\varrho,h}u-\mathscr{R}^{m[\beta]}_{\varrho,h}\|_{H^{|\gamma|}(\Omega)} = \|\left(u-\mathscr{R}^{m[0]}_{\varrho,h}u\right)+\left(\rho^\beta D^\beta_x u-\mathscr{R}^{m[\beta]}_{\varrho,h}\right)-\rho^\beta D^\beta_x u\|_{H^{|\gamma|}(\Omega)}$$

†† Readers may find useful information on vanishing moments condition of a wavelet, or multiplicity zero condition of its Fourier transform, and its effect on bandwidth in [16, pp. 243–245]

$$\leqslant \|u-\mathscr{R}_{\varrho,h}^{m[0]}u\|_{H^{m+1}(\Omega)}+\|\rho^{\beta}D_x^{\beta}u-\mathscr{R}_{\varrho,h}^{m[\beta]}u\|_{H^{m+1}(\Omega)}+\rho^{|\beta|}\|D_x^{\beta}u\|_{H^{|\gamma|}(\Omega)}$$
$$\leqslant C_1\rho^{m+1-|\gamma|}\|u\|_{H^{m+1}(\Omega)}+C_2\rho^{m+1-|\gamma|}\|u\|_{H^{m+1}(\Omega)}+C_3\rho^{p}\|u\|_{H^{m+1}(\Omega)} \tag{87}$$

Note that in the last step, we use the fact that $\|u\|_{H^{m+1}(\Omega)} \hookrightarrow \|D^{\beta}u\|_{H^{|\gamma|}(\Omega)}$ because $|\beta+\gamma| \leqslant m+1$. Furthermore, considering the fact $0<|\beta| \leqslant m+1-|\gamma| \Rightarrow 0 \leqslant |\gamma| \leqslant m+1-|\beta|$, we have the desired result

$$\|u-\mathscr{R}_{\varrho,h}^{m[s]}u\|_{H^{|\gamma|}(\Omega)} \leqslant C_4\rho^{p}\|u\|_{H^{m+1}(\Omega)} \tag{88}$$

□

4.4. An heuristic explanation of synchronized convergence

As a matter of fact, the synchronized reproducing kernel, $\mathscr{K}_{\varrho}^{[s]}(\cdot,\cdot)=\mathscr{K}_{\varrho}^{[0]}(\cdot,\cdot)+C_{\beta}\mathscr{K}_{\varrho}^{[\beta]}(\cdot,\cdot)$, satisfies the following differential consistency condition:

$$\sum_{I\in\Lambda}\left(\frac{x_I-x}{\varrho}\right)^{\alpha}D_{x/\rho}^{\gamma}\mathscr{K}_{\varrho}^{[s]}(x_I-x,x)\Delta V_I=\alpha!\delta_{\alpha\gamma}+\frac{\alpha!}{(\alpha-\gamma)!}\delta_{\alpha(\beta+\gamma)}C_{\beta} \tag{89}$$

which can be written in terms of moment equations

$$M_{\alpha}^{[s](\gamma)}=\alpha!\delta_{\alpha\gamma}+\frac{\alpha!}{\beta!}\delta_{\alpha(\beta+\gamma)}C_{\beta} \tag{90}$$

where $M_{\alpha}^{[s]}:=M_{\alpha}^{[0]}+C_{\beta}M_{\alpha}^{[\beta]}$.

This synchronized convergence phenomenon is basically the consequence of the differential consistency condition (89). For a better insight, it would be beneficial to examine the effect of the differential consistency condition (89) on the pointwise truncation error of the interpolant approximation. Consider the case that $C_{\alpha}=0,\ \forall\alpha\neq 0,\beta$. We expand (85) via Taylor expansion,

$$\mathscr{R}_{\varrho,h}^{m[s]}u(x)=\sum_{I\in\Lambda}\mathscr{K}_{\varrho}^{[s]}(x_I-x,x)\left\{u(x)+u^{(1)}(x)(x_I-x)+\frac{1}{2!}u^{(2)}(x)(x_I-x)^2+\cdots\right\}\Delta V_I$$
$$=u(x)M_0^{[s]}(x)+\varrho u^{(1)}(x)M_1^{[s]}(x)+\frac{\varrho^2}{2!}u^{(2)}(x)M_2^{[s]}(x)+\frac{\varrho^3}{3!}u^{(3)}(x)M_3^{[s]}(x)$$
$$+\frac{\varrho^4}{4!}u^{(4)}(x)M_4^{[s]}(x)+\mathscr{O}(\varrho^5) \tag{91}$$

where

$$u^{(n)}(x):=D_x^n u(x) \tag{92}$$

Proceeding similarly, one may derive further

$$D_x\{\mathscr{R}_{\varrho,h}^{m[s]}u(x)\}=\sum_{I\in\Lambda}D_x\mathscr{K}_{\varrho}^{[s]}(x_I-x,x)u(x_I)\Delta V_I$$
$$=\frac{1}{\varrho}u(x)M_0^{[s](1)}(x)+u^{(1)}(x)M_1^{[s](1)}(x)+\frac{\varrho}{2!}u^{(2)}(x)M_2^{[s](1)}(x)$$
$$+\frac{\varrho^2}{3!}u^{(3)}(x)M_3^{[s](1)}(x)+\frac{\varrho^3}{4!}u^{(4)}(x)M_4^{[s](1)}(x)+\mathscr{O}(\varrho^4) \tag{93}$$

Table V. Differential consistency conditions for the zero-th-order $\mathscr{K}_\varrho^{[s]}$

$M_4^{[0]} \neq 0$	$M_4^{[0](1)} \neq 0$	$M_4^{[0](2)} \neq 0$	$M_4^{[0](3)} \neq 0$
$M_3^{[0]} = 0$	$M_3^{[0](1)} = 0$	$M_3^{[0](2)} = 0$	$M_3^{[0](3)} = 3!$
$M_2^{[0]} = 0$	$M_2^{[0](1)} = 0$	$M_2^{[0](2)} = 2!$	$M_2^{[0](3)} = 0$
$M_1^{[0]} = 0$	$M_1^{[0](1)} = 1!$	$M_1^{[0](2)} = 0$	$M_1^{[0](3)} = 0$
$M_0^{[0]} = 0!$	$M_0^{[0](1)} = 0$	$M_0^{[0](2)} = 0$	$M_0^{[0](3)} = 0$

where

$$M_i^{[s](j)}(x) := \sum_{I \in \Lambda} \left(\frac{x_I - x}{\varrho} \right)^i D_{x/\varrho}^j \mathscr{K}_\varrho^{[s]}(x_I - x, x) \Delta V_I$$

and

$$\begin{aligned} D_x^2 \{ \mathscr{R}_{\varrho,h}^{m[s]} u(x) \} &= \sum_{I \in \Lambda} D_x^2 \mathscr{K}_\varrho^{[s]}(x_I - x, x) u(x_I) \Delta V_I \\ &= \frac{1}{\varrho^2} u(x) M_0^{[s](2)}(x) + \frac{1}{\varrho} u^{(1)}(x) M_1^{[s](2)}(x) + \frac{1}{2!} u^{(2)}(x) M_2^{[s](2)}(x) \\ &\quad + \frac{\varrho}{3!} u^{(3)}(x) M_3^{[s](2)}(x) + \frac{\varrho^2}{4!} u^{(4)}(x) M_4^{[s](2)}(x) + \mathscr{O}(\varrho^3) \end{aligned} \tag{94}$$

$$\begin{aligned} D_x^3 \{ \mathscr{R}_{\varrho,h}^{m[s]} u(x) \} &= \sum_{I \in \Lambda} D_x^3 \mathscr{K}_\varrho^{[s]}(x_I - x, x) u(x_I) \Delta V_I \\ &= \frac{1}{\varrho^3} u(x) M_0^{[s](3)}(x) + \frac{1}{\varrho^2} u^{(1)}(x) M_1^{[s](3)}(x) + \frac{1}{2!\varrho} u^{(2)}(x) M_2^{[s](3)}(x) \\ &\quad + \frac{1}{3!} u^{(3)}(x) M_3^{[s](3)}(x) + \frac{\varrho}{4!} u^{(4)}(x) M_4^{[s](3)}(x) + \mathscr{O}(\varrho^2) \end{aligned} \tag{95}$$

In Tables V and VI, we tabulate both the differential consistency conditions of the first-order SRK interpolant and the truncation errors for the case $m = 3,\ p = 1$. In Table VI, there is a shaded ladder lying through the truncation errors at the order $\mathscr{O}(\varrho)$. Comparing between Tables V and VI, all the quantities below the shaded ladder are zero, and the quantities on the ladder are non-zero. As a matter of fact, Table V indicates that $M_1^{[s]} = 1!C_1, M_2^{[s](1)} = 2!C_1,\ M_3^{[s](2)} = 3!C_1$ and of course $M_4^{[s](3)} \neq 0$ in general. This shows clearly that all the truncation errors are synchronized. In parallel, there is a shaded ladder locating along the line where all the truncation errors are at order $\mathscr{O}(\varrho^1)$. By the same token, all the entries below the shaded ladder are zero, whereas the entries on the shaded ladder are non-zero. Again, all the relevant truncation errors are synchronized. This synchronized pattern of truncation error has an one-to-one correspondence with the global interpolation error estimate. In Tables VII and VIII, the differential consistent condition of the second-order SRK interpolant and the associated truncation errors are tabulated.

Table VI. Pointwise truncation error for the zeroth-order SRK interpolant

$u-\mathscr{R}^{m[s]}_{\varrho,h}u=$	$u\left(1-M_0^{[0]}\right)$	$-\varrho u^{(1)}M_1^{[0]}$	$-\frac{\varrho^2}{2!}u^{(2)}M_2^{[0]}$	$-\frac{\varrho^3}{3!}u^{(3)}M_3^{[0]}$	$-\frac{\varrho^4}{4!}u^{(4)}M_4^{[0]}$
	0	0	0	0	$\mathscr{O}(\varrho^4)$
$D_x\left(u-\mathscr{R}^{m[s]}_{\varrho,h}u\right)=$	$-\frac{1}{\varrho}uM_0^{[0](1)}$	$u^{(1)}\left(1-M_1^{[0](1)}\right)$	$-\frac{\varrho}{2!}u^{(2)}M_2^{[0](1)}$	$-\frac{\varrho^2}{3!}u^{(3)}M_3^{[0](1)}$	$-\frac{\varrho^3}{4!}u^{(4)}M_4^{[0](1)}$
	0	0	0	0	$\mathscr{O}(\varrho^3)$
$D_x^2\left(u-\mathscr{R}^{m[s]}_{\varrho,h}u\right)=$	$-\frac{1}{\varrho^2}uM_0^{[0](2)}$	$-\frac{1}{\varrho}u^{(1)}M_1^{[0](2)}$	$u^{(2)}\left(1-\frac{1}{2!}M_2^{[0](2)}\right)$	$-\frac{\varrho}{3!}u^{(3)}M_3^{[0](2)}$	$-\frac{\varrho^2}{4!}u^{(4)}M_4^{[0](2)}$
	0	0	0	0	$\mathscr{O}(\varrho^2)$
$D_x^3\left(u-\mathscr{R}^{m[s]}_{\varrho,h}u\right)=$	$-\frac{1}{\varrho^3}uM_0^{[0](3)}$	$-\frac{1}{\varrho^2}u^{(1)}M_1^{[0](3)}$	$-\frac{1}{2!\varrho}u^{(2)}M_2^{[0](3)}$	$u^{(3)}\left(1-\frac{1}{3!}M_3^{[0](3)}\right)$	$-\frac{\varrho}{4!}u^{(4)}M_4^{[0](3)}$
	0	0	0	0	$\mathscr{O}(\varrho)$

Table VII. Differential consistency conditions for the second-order $\mathscr{K}^{[s]}_{\varrho}$

$M_3^{[s]}=0$	$M_3^{[s](1)}=3!/2!C_2$	$M_3^{[s](2)}=0$	$M_3^{[s](3)}=3!$
$M_2^{[s]}=1!C_2$	$M_2^{[s](1)}=0$	$M_2^{[s](2)}=2!$	$M_2^{[s](3)}=0$
$M_1^{[s]}=0$	$M_1^{[s](1)}=1!$	$M_1^{[s](2)}=0$	$M_1^{[s](3)}=0$
$M_0^{[s]}=0!$	$M_0^{[s](1)}=0$	$M_0^{[s](2)}=0$	$M_0^{[s](3)}=0$

Table VIII. Pointwise truncation error for the second-order SRK interpolant

$u-\mathscr{R}^{m[s]}_{\varrho,h}u=$	$u\left(1-M_0^{[s]}\right)$	$-\varrho u^{(1)}M_1^{[s]}$	$-\frac{\varrho^2}{2!}u^{(2)}M_2^{[s]}$	$-\frac{\varrho^3}{3!}u^{(3)}M_3^{[s]}$	$-\frac{\varrho^4}{4!}u^{(4)}M_4^{[s]}$
	0	0	$\mathscr{O}(\varrho^2)$	$\mathscr{O}(\varrho^3)$	$\mathscr{O}(\varrho^4)$
$D_x\left(u-\mathscr{R}^{m[s]}_{\varrho,h}u\right)=$	$-\frac{1}{\varrho}uM_0^{[s](1)}$	$u^{(1)}\left(1-M_1^{[s](1)}\right)$	$-\frac{\varrho}{2!}u^{(2)}M_2^{[s](1)}$	$-\frac{\varrho^2}{3!}u^{(3)}M_3^{[s](1)}$	$-\frac{\varrho^3}{4!}u^{(4)}M_4^{[s](1)}$
	0	0	0	$\mathscr{O}(\varrho^2)$	$\mathscr{O}(\varrho^3)$
$D_x^2\left(u-\mathscr{R}^{m[s]}_{\varrho,h}u\right)=$	$-\frac{1}{\varrho^2}uM_0^{[s](2)}$	$-\frac{1}{\varrho}u^{(1)}M_1^{[s](2)}$	$u^{(2)}\left(1-\frac{1}{2!}M_2^{[s](2)}\right)$	$-\frac{\varrho}{3!}u^{(3)}M_3^{[s](2)}$	$-\frac{\varrho^2}{4!}u^{(4)}M_4^{[s](2)}$
	0	0	0	0	$\mathscr{O}(\varrho^2)$

Numerical experiments have been conducted to verify the theoretical claim. By using the synchronized reproducing kernel discussed in Example 3.1, we interpolate function $u(x)=\sin(x)$ in a 1-D segment $[0,1]$, and the numerical results are exhibited in Figure 5. In Figure 5, there are two cases. In the case (a), $p=1$ and $\gamma=0,1,2,3$, which means that the interpolation error norm L^2, H^1, H^2, and H^3 are all having the same convergence rate at order 1. This corresponds exactly to the synchronized truncation errors shown in Table VI. In the case (b), $p=2$ and $\gamma=0,1,2,$

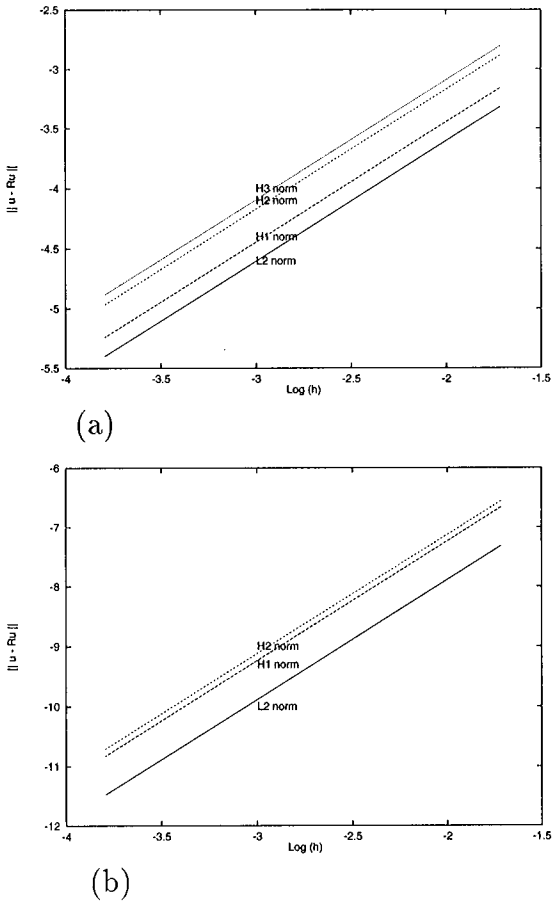

Figure 5. Synchronized convergence rates: (a) $m=3$, $p=1$, $\gamma=0,1,2,3$; (b) $m=3$; $p=2$; $\gamma=0,1,2$

which means that the convergence rates of the interpolation errors of the norm L^2, H^1, and H^2, are all synchronized at order $p=2$.

5. WAVELET-LIKE FUNCTIONS AND WAVELET KERNEL PACKET

In this section, we present some examples of wavelet-like shape functions, and wavelet kernel packet. Once again, the term 'wavelet kernel packet' is referred to as 'a group of distinct basic wavelet functions', which may not necessarily provide a group of orthogonal wavelet basis in $L(\mathbb{R})^n$. For the sake of simplicity, it is always assumed that $\Omega=\mathbb{R}$ and $\phi\in H^s(\mathbb{R})$, $s>m+1$. In the following, only 1-D hierarchical reproducing kernel functions in continuous form are considered, unless otherwise stated. Contrast to the discrete cases in Section 3, all the moments of the window function are constant here, and the vector, $\mathbf{b}^{(\alpha)}$, is a constant as well; thus,

$$\mathscr{K}^{[\alpha]}(y,x)\equiv\mathscr{K}^{[\alpha]}(y),\quad \forall\alpha\geqslant 0. \tag{96}$$

For the particular purpose, denote the αth mth-order hierarchical reproducing kernels as $\psi_m^{[\alpha]}(x) = \mathscr{K}^{[\alpha]}(x)$. By construction,

$$\int_{\mathbb{R}} x^\alpha \psi_m^{[\beta]}(x)\,\mathrm{d}x = \delta_{\alpha\beta}, \quad \beta \leqslant m \tag{97}$$

For $\beta \neq 0$, $\psi^\beta(x)$ satisfies $(m-1)$th order vanishing moment conditions, i.e.

$$\int_{-\infty}^{\infty} \psi_m^{[\beta]}(x)\,\mathrm{d}x = 0 \quad \text{and} \quad \int_{-\infty}^{\infty} x^\alpha \psi_m^{[\beta]}(x)\,\mathrm{d}x = 0, \quad \alpha \neq \beta \tag{98}$$

In general, $\{\psi_m^{[\alpha]}(\cdot - k)\}_{k\in\mathbf{Z}}$ may not be an orthogonal sequence. Nevertheless, it possesses some special properties. Some preliminary results of these special properties are discussed by the following examples.

Example 5.1. In this example, the linear B-spline is chosen as the window function, which has a compact support in $|x| \leqslant 1$.

$$\phi(x) = \begin{cases} 1 - |x|, & |x| \leqslant 1 \\ 0 & \text{otherwise} \end{cases} \tag{99}$$

The linear generating polynomial basis $\mathbf{P}(x) = (1, x)$ is used in the construction. The expression of the kernel function is $\psi_1^{[\alpha]}(x) = \mathbf{P}(x)\mathbf{b}^{(\alpha)}\phi(x)$, where vectors $\mathbf{b}^\alpha$ satisfy the moment equation

$$\begin{pmatrix} m_0 & m_1 \\ m_1 & m_2 \end{pmatrix} \begin{pmatrix} b_1^{(\alpha)} \\ b_2^{(\alpha)} \end{pmatrix} = \begin{pmatrix} \delta_{\alpha 0} \\ \delta_{\alpha 1} \end{pmatrix} \tag{100}$$

Simple calculation shows that $m_0 = 1$, $m_1 = 0$, $m_2 = 1/6$. Subsequently, it is obtained that $\mathbf{b}_1^{(0)} = (1, 0)^{\mathrm{t}}$, $\mathbf{b}_1^{(1)} = (0, 6)^{\mathrm{t}}$ and

$$\psi_1^{[0]}(x) = m_0^{-1}\phi(x) = \phi(x) \tag{101}$$

$$\psi_1^{[1]}(x) = m_2^{-1}x\phi(x) = 6x\phi(x) \tag{102}$$

The wavelet kernel packet is depicted in Figure 6. One may verify the orthogonality condition

$$\int_{\infty}^{\infty} \psi_1^{[0]}(x)\psi_1^{[1]}(x)\,\mathrm{d}x = \int_{-1}^{1} 6x\phi^2(x)\,\mathrm{d}x = 0 \tag{103}$$

Example 5.2. In this example, the standard Gaussian function

$$g_\sigma(x) = \frac{1}{2\sqrt{\pi\sigma}} \exp\left\{-\frac{x^2}{4\sigma}\right\} \tag{104}$$

is chosen as the window function. Let the generating polynomial vector $\mathbf{P}(x) = (1, x, x^2, x^3)$, i.e. $m = 3$. The wavelet kernel packet is then described as $\psi_3^{[\alpha]}(x) = \mathbf{P}(x)\mathbf{b}^{(\alpha)}g_\sigma(x)$, where the vectors

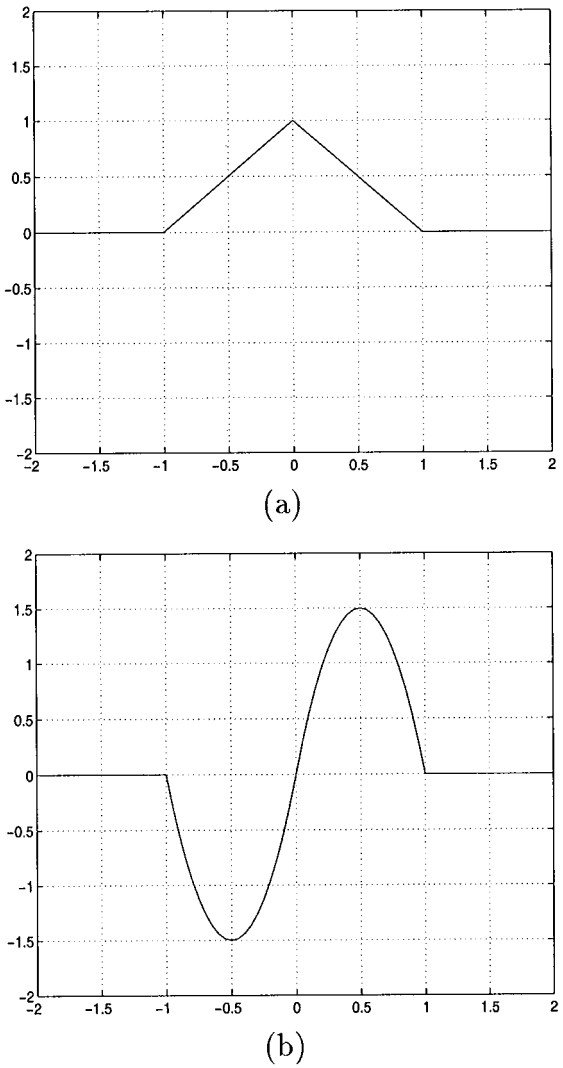

Figure 6. The first-order wavelet kernel packet: (a) $\psi_1^{[0]}(x)$;(b) $\psi_1^{[1]}(x)$

$\mathbf{b}^{(\alpha)}$ are the solutions of the global moment equation

$$\begin{pmatrix} m_0 & 0 & m_2 & 0 \\ 0 & m_2 & 0 & m_4 \\ m_2 & 0 & m_4 & 0 \\ 0 & m_4 & 0 & m_6 \end{pmatrix} \begin{pmatrix} b_1^{(\alpha)} \\ b_2^{(\alpha)} \\ b_3^{(\alpha)} \\ b_4^{(\alpha)} \end{pmatrix} = \begin{pmatrix} \delta_{\alpha 0} \\ \delta_{\alpha 1} \\ \delta_{\alpha 2} \\ \delta_{\alpha 3} \end{pmatrix} \tag{105}$$

Since the solution space of the above system equations can be decomposed into two invariant subspaces, in turn, equation (105) can be reduced into two lower-order linear algebraic

equations:

$$\begin{pmatrix} m_0 & m_2 \\ m_2 & m_4 \end{pmatrix} \begin{pmatrix} b_1^{(\alpha)} \\ b_3^{(\alpha)} \end{pmatrix} = \begin{pmatrix} \delta_{\alpha 0} \\ \delta_{\alpha 2} \end{pmatrix}, \quad |\alpha| \text{ is even} \tag{106}$$

with $b_1^{(\alpha)} = b_4^{(\alpha)} = 0$. And

$$\begin{pmatrix} m_0 & m_2 \\ m_2 & m_4 \end{pmatrix} \begin{pmatrix} b_2^{(\alpha)} \\ b_4^{(\alpha)} \end{pmatrix} = \begin{pmatrix} \delta_{\alpha 1} \\ \delta_{\alpha 3} \end{pmatrix}, \quad |\alpha| \text{ is odd} \tag{107}$$

with $b_1^{(\alpha)} = b_3^{(\alpha)} = 0$. The components of the wavelet kernel packet are

$$\psi_3^{[0]}(x) = \left(\frac{3}{2} - \frac{x^2}{4\sigma}\right) g_\sigma(x) \tag{108}$$

$$\psi_3^{[1]}(x) = \frac{x}{4\sigma}\left(5 - \frac{x^2}{2\sigma}\right) g_\sigma(x) \tag{109}$$

$$\psi_3^{[2]}(x) = \frac{1}{4\sigma}\left(\frac{x^2}{2\sigma} - 1\right) g_\sigma(x) \tag{110}$$

$$\psi_3^{[3]}(x) = \frac{x}{8\sigma^2}\left(\frac{x^2}{6\sigma} - 1\right) g_\sigma(x) \tag{111}$$

One can verify the orthogonality conditions:

$$\int_{-\infty}^{\infty} \psi_3^{[0]}(x)\psi_3^{[1]}(x)\,\mathrm{d}x = \int_{-\infty}^{\infty} \psi_3^{[0]}(x)\psi_3^{[3]}(x)\,\mathrm{d}x = \int_{-\infty}^{\infty} \psi_3^{[2]}(x)\psi_3^{[1]}(x)\,\mathrm{d}x$$
$$= \int_{-\infty}^{\infty} \psi_3^{[2]}(x)\psi_3^{[3]}(x)\,\mathrm{d}x = 0$$

However, in general, $\int_{-\infty}^{\infty} \psi_3^{[0]}(x)\psi_3^{[1]}(x-k)\,\mathrm{d}x \neq 0,\ k \in \mathbf{Z}$. This means that the wavelet sequences constructed here do not form a discrete orthogonal bases. Figure 7 displays each member of the basic wavelet function packet.

Example 5.3. Let $m=4$, $\mathbf{P}(x)=(1,x,x^2,x^3,x^4)$, and $\psi_4^{[\alpha]}(x) = \mathbf{P}(x)\mathbf{b}^{(\alpha)}\phi(x)$. As long as the window function is selected to be symmetric with respect to the y-axis ($x=0$), the moment matrix has an alternative mode with zero and non-zero entries; this is because all the odd order moments are zero. In this case, one has

$$\mathbf{M} = \begin{pmatrix} m_0 & 0 & m_2 & 0 & m_4 \\ 0 & m_2 & 0 & m_4 & 0 \\ m_2 & 0 & m_4 & 0 & m_6 \\ 0 & m_4 & 0 & m_6 & 0 \\ m_4 & 0 & m_6 & 0 & m_8 \end{pmatrix} \tag{112}$$

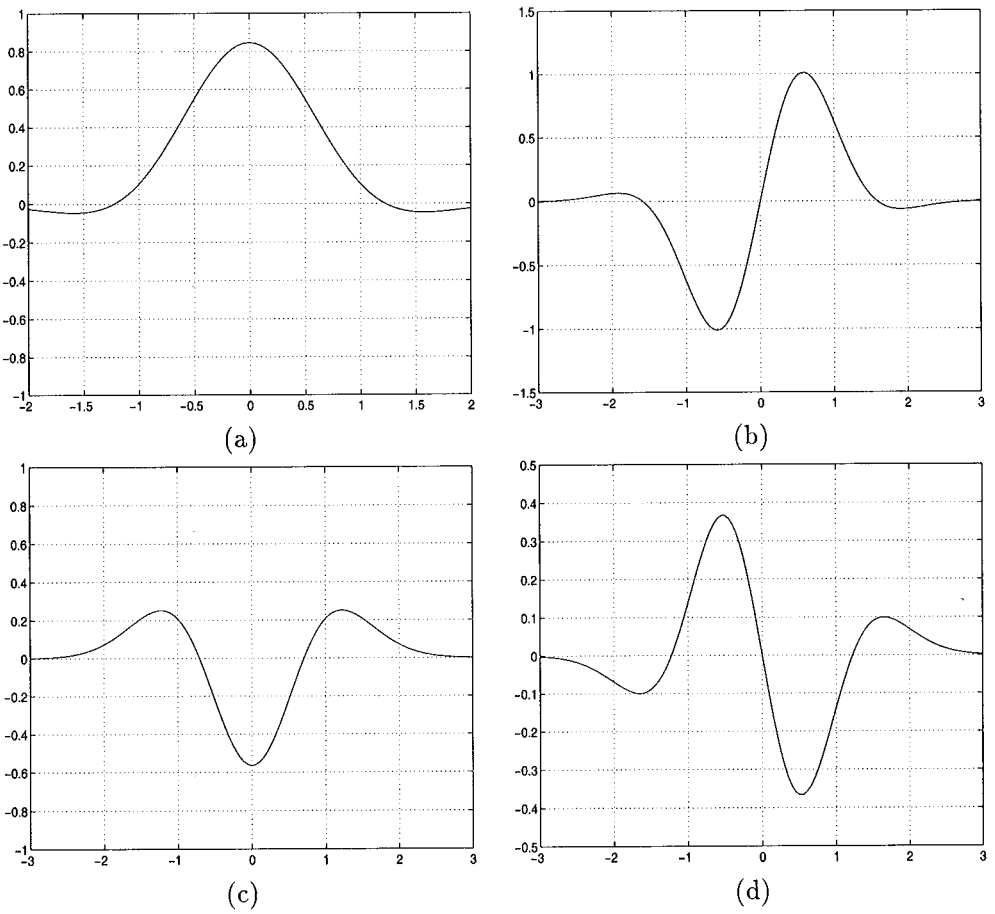

Figure 7. An third-order wavelet kernel packet: (a) $\psi_3^{[0]}(x)$; (b) $\psi_3^{[1]}(x)$; (c) $\psi_3^{[2]}(x)$; (d) $\psi_3^{[3]}(x)$

Consequently, the moment matrix is reducible. Then the vectors $\mathbf{b}^{(\alpha)}$ can be determined by two separated systems of equations:

$$\begin{pmatrix} m_0 & m_2 & m_4 \\ m_2 & m_4 & m_6 \\ m_4 & m_6 & m_8 \end{pmatrix} \begin{pmatrix} b_1^{(\alpha)} \\ b_3^{(\alpha)} \\ b_4^{(\alpha)} \end{pmatrix} = \begin{pmatrix} \delta_{\alpha 0} \\ \delta_{\alpha 2} \\ \delta_{\alpha 4} \end{pmatrix}, \quad |\alpha| \text{ is even} \tag{113}$$

with $b_2^{(\alpha)} = b_4^{(\alpha)} = 0$. And

$$\begin{pmatrix} m_2 & m_4 \\ m_4 & m_6 \end{pmatrix} \begin{pmatrix} b_2^{(\alpha)} \\ b_4^{(\alpha)} \end{pmatrix} = \begin{pmatrix} \delta_{\alpha 1} \\ \delta_{\alpha 3} \end{pmatrix}, \quad |\alpha| \text{ is odd} \tag{114}$$

with $b_1^{(\alpha)} = b_3^{(\alpha)} = b_5^{(\alpha)} = 0$.

By choosing the Gaussian function as the window function, the explicit solutions for this particular wavelet kernel packet are as follows:

$$\psi_4^{[0]}(x) = \left(\frac{15}{8} - \frac{5x^2}{8\sigma} + \frac{x^4}{32\sigma^2}\right) g_\sigma(x) \tag{115}$$

$$\psi_4^{[1]}(x) = \frac{x}{4\sigma}\left(5 - \frac{x^2}{2\sigma}\right) g_\sigma(x) \tag{116}$$

$$\psi_4^{[2]}(x) = \left(-\frac{5}{8\sigma} + \frac{x^2}{2\sigma^2} - \frac{x^4}{32\sigma^3}\right) g_\sigma(x) \tag{117}$$

$$\psi_4^{[3]}(x) = \frac{x}{8\sigma^2}\left(-1 + \frac{x^2}{6\sigma}\right) g_\sigma(x) \tag{118}$$

$$\psi_4^{[4]}(x) = \left(\frac{1}{32\sigma^2} - \frac{x^2}{32\sigma^3} + \frac{x^4}{384\sigma^4}\right) g_\sigma(x) \tag{119}$$

All members of the wavelet kernel packet are shown in Figure 8. In Figure 8(f), a synchronized reproducing kernel interpolant is plotted, which is constructed based on the formula, $\mathscr{K}^{[s]}(x) = \psi_4^{[0]}(x) - 0{\cdot}5\psi_4^{[1]}(x)$, which shows the upwind feature.

In general, if one chooses a symmetric window function $\phi \in H^s(\mathbb{R})$ in the construction process, for the even-order moment matrix ($m = 2n - 1$ and $\ell = 2n$), the global moment matrix will have the form

$$\mathbf{M} = \begin{pmatrix} m_0 & 0 & m_2 & 0 & \cdots & m_{2n-2} & 0 \\ 0 & m_2 & 0 & \cdots & & 0 & m_{2n} \\ m_2 & 0 & \ddots & & & m_{2n} & \vdots \\ \vdots & & & \ddots & & & \vdots \\ \vdots & & & & \ddots & & \vdots \\ m_{2n-2} & 0 & & & & \ddots & 0 \\ 0 & m_{2n} & \cdots & & \cdots & 0 & m_{2\ell} \end{pmatrix} \tag{120}$$

The system of equations, $\mathbf{M}\mathbf{b}^{(\alpha)} = \{\mathbf{P}^{(\alpha)}(0)\}^{\mathrm{t}}$, can then be broken down into two sets of order n linear algebraic equations. They are

$$\begin{pmatrix} m_0 & m_2 & \cdots & m_{2n-2} \\ m_2 & m_4 & & m_{2n} \\ \vdots & & \ddots & \vdots \\ m_{2n-2} & m_{2n} & \cdots & m_{2\ell-2} \end{pmatrix} \begin{pmatrix} b_1^{(\alpha)} \\ b_3^{(\alpha)} \\ \vdots \\ b_{2n-1}^{(\alpha)} \end{pmatrix} = \begin{pmatrix} \delta_{\alpha 0} \\ \delta_{\alpha 2} \\ \vdots \\ \delta_{\alpha(2n-2)} \end{pmatrix}, \quad \alpha = \text{even} \tag{121}$$

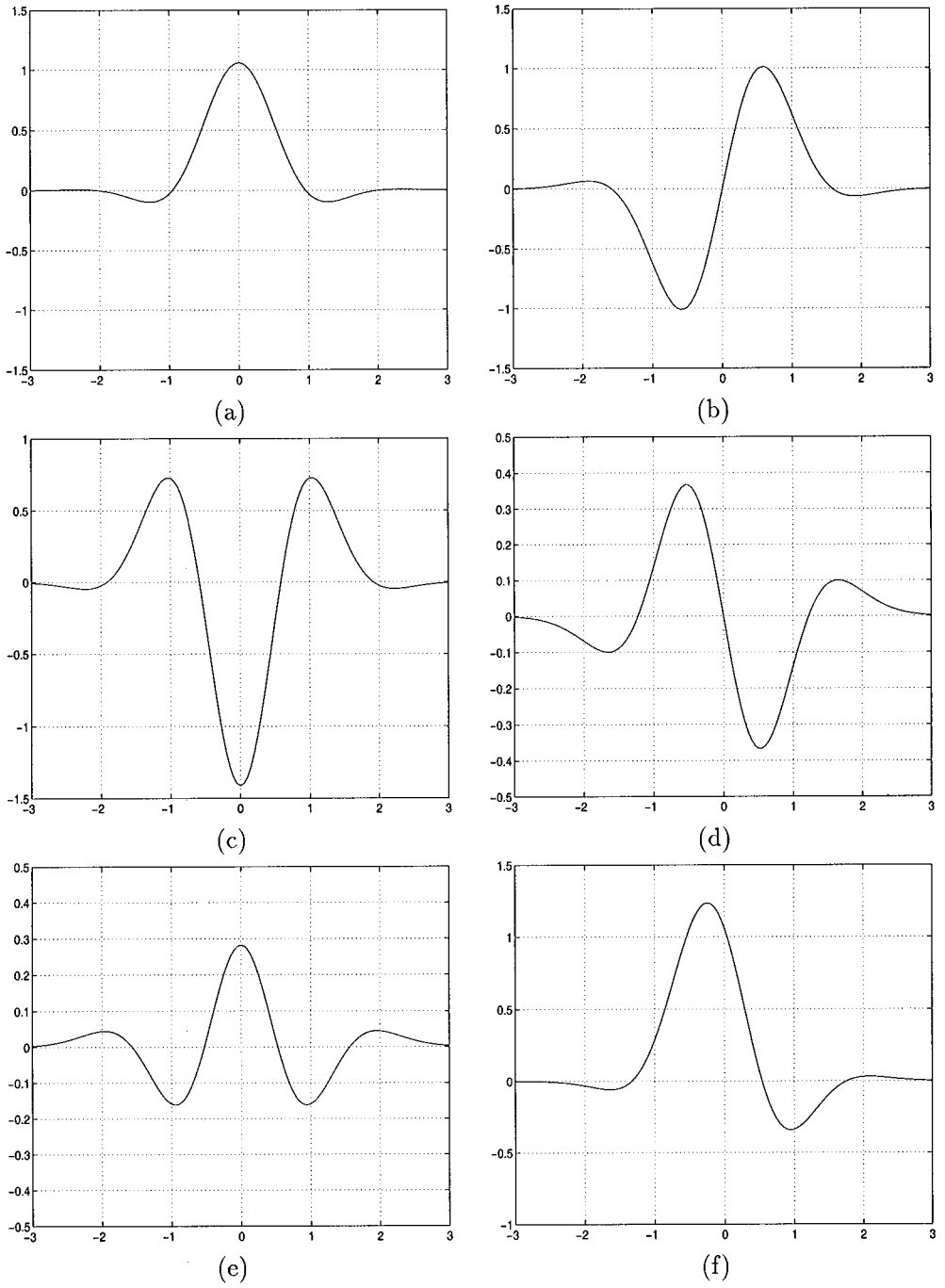

Figure 8. An fourth-order wavelet kernel packet: (a) $\psi_4^{[0]}(x)$; (b) $\psi_4^{[1]}(x)$; (c) $\psi_4^{[2]}(x)$; (d) $\psi_4^{[3]}(x)$; (e) $\psi_4^{[4]}(x)$; (f) $\mathscr{K}^{[s]}(x)$

with $b_2^{(\alpha)} = b_4^{(\alpha)} = \cdots = b_{2n}^{(\alpha)} = 0$, and

$$\begin{pmatrix} m_2 & m_4 & \cdots & m_{2n} \\ m_4 & m_6 & & m_{2n+2} \\ \vdots & & \ddots & \vdots \\ m_{2n} & m_{2n+2} & \cdots & m_{2\ell} \end{pmatrix} \begin{pmatrix} b_2^{(\alpha)} \\ b_4^{(\alpha)} \\ \vdots \\ b_{2n}^{(\alpha)} \end{pmatrix} = \begin{pmatrix} \delta_{\alpha 1} \\ \delta_{\alpha 3} \\ \vdots \\ \delta_{\alpha(2n-1)} \end{pmatrix}, \quad |\alpha| \text{ is odd} \tag{122}$$

with $b_1^{(\alpha)} = b_3^{(\alpha)} = \cdots = b_{2n-1}^{(\alpha)} = 0$.

The corresponding wavelet solutions can be shown as

$$\psi_{2n-1}^{[2j-2]}(x) = \frac{1}{\Delta}\{A_{(2j-1)1} + A_{(2j-1)3}x^2 + \cdots + A_{(2j-1)(2n-1)}x^{2n-2}\}\phi(x)$$

$$\psi_{2n-1}^{[2j-1]}(x) = \frac{1}{\Delta}\{A_{(2j)2}x + A_{(2j)4}x^3 + \cdots + A_{(2j)(2n)}x^{2n-1}\}\phi(x)$$

where $j = 1, \ldots, n$, and A_{ij} are the cofactors of the global matrix $\mathbf{M}$ and $\Delta := \det \mathbf{M}$. By the symmetry argument, it is obvious that

$$\int_{-\infty}^{\infty} \psi_{2n-1}^{[\alpha]}(x)\psi_{2n-1}^{[\beta]}(x)\,\mathrm{d}x = 0, \quad |\alpha| \text{ is odd, } |\beta| \text{ is even} \tag{123}$$

For the odd-order global moment matrix ($m = 2n$ and $\ell = 2n + 1$),

$$\mathbf{M} = \begin{pmatrix} m_0 & 0 & m_2 & 0 & \cdots & 0 & m_{2n} \\ 0 & m_2 & 0 & \cdots & & m_{2n} & 0 \\ m_2 & 0 & \ddots & & & 0 & \vdots \\ \vdots & & & \ddots & & & \vdots \\ \vdots & & & & \ddots & & \vdots \\ 0 & m_{2n} & & & & \ddots & 0 \\ m_{2n} & 0 & \cdots & & \cdots & 0 & m_{2\ell} \end{pmatrix} \tag{124}$$

the system of equations breaks into two unequal order systems of equations:

$$\begin{pmatrix} m_0 & m_2 & \cdots & m_{2n} \\ m_2 & m_4 & & m_{2n+2} \\ \vdots & & \ddots & \vdots \\ m_{2n} & m_{2n+2} & \cdots & m_{2\ell} \end{pmatrix} \begin{pmatrix} b_1^{(\alpha)} \\ b_3^{(\alpha)} \\ \vdots \\ b_{2n+1}^{(\alpha)} \end{pmatrix} = \begin{pmatrix} \delta_{\alpha 0} \\ \delta_{\alpha 2} \\ \vdots \\ \delta_{\alpha(2n)} \end{pmatrix}, \quad |\alpha| \text{ is even} \tag{125}$$

with $b_2^{(\alpha)} = b_4^{(\alpha)} = \cdots = b_{2n}^{(\alpha)} = 0$, and

$$\begin{pmatrix} m_2 & m_4 & \cdots & m_{2n} \\ m_2 & m_4 & & m_{2n+2} \\ \vdots & & \ddots & \vdots \\ m_{2n} & m_{2n+2} & \cdots & m_{4n} \end{pmatrix} \begin{pmatrix} b_2^{(\alpha)} \\ b_4^{(\alpha)} \\ \vdots \\ b_{2n}^{(\alpha)} \end{pmatrix} = \begin{pmatrix} \delta_{\alpha 1} \\ \delta_{\alpha 3} \\ \vdots \\ \delta_{\alpha(2n-1)} \end{pmatrix}, \quad |\alpha| \text{ is odd} \tag{126}$$

with $b_1^{(\alpha)} = b_3^{(\alpha)} = \cdots = b_{2n+1}^{(\alpha)} = 0$.

The corresponding solutions for the pre-wavelet sequence are

$$\psi_{2n}^{[2j+1]}(x) = \frac{1}{\Delta}\{A_{(2j)2}x + A_{(2j)4}x^3 + \cdots + A_{(2j)(2n)}x^{2n-1}\}\phi(x)$$
$$\psi_{2n}^{[2j]}(x) = \frac{1}{\Delta}\{A_{(2j+1)1} + A_{(2j+1)3}x^2 + \cdots + A_{(2j+1)(2n+1)}x^{2n}\}\phi(x)$$

where $j = 0, 1, \ldots, n$. As mentioned at the beginning, the wavelet packet derived here are a group of basic, or mother wavelets, which may not form an orthogonal wavelet basis in $L^2(\mathbb{R})$,[‡‡] i.e. they are only pre-wavelets. That is, in an uniform lattice, $k \in \mathbf{Z}$,

$$\int_{-\infty}^{\infty} \psi_m^{[\alpha]}(x)\psi_m^{[\alpha]}(x-k)\,\mathrm{d}x \neq 0, \quad \int_{-\infty}^{\infty} \psi_m^{[\alpha]}(x)\psi_m^{[\beta]}(x-k)\,\mathrm{d}x \neq 0 \tag{127}$$

However, the situation in (127) can be improved. If specific window function is carefully selected. A simple example of such construction is to use a symmetric orthogonal window function, i.e. a function satisfies: $\phi(x) = \phi(-x)$ and $\sum_{k=-\infty}^{\infty} |\hat{\phi}(\zeta + 2\pi k)|^2 = 1$. Let us consider the wavelet basis discussed in Example 5.11. There are two components in the packet: $\psi_1^{[0]} = m_0^{-1}\phi(x)$ and $\psi_1^{[1]} = m_2^{-1}x\phi(x)$. By utilizing the Parseval identity, simple calculation shows that $\forall j \in \mathbf{Z}$,

$$\begin{aligned} \int_{-\infty}^{\infty} \psi_1^{[0]}(x)\psi_1^{[1]}(x-j)\,\mathrm{d}x &= m_0^{-1}m_2^{-1}\int_{-\infty}^{\infty} \phi(x)(x-j)\phi(x-j)\,\mathrm{d}x \\ &= \frac{i}{2\pi(m_0 m_2)}\int_{-\infty}^{\infty} \hat{\phi}(\zeta)\hat{\phi}'(\zeta)\exp(-ij\zeta)\,\mathrm{d}\zeta \\ &= \frac{i}{4\pi(m_0 m_2)}\int_{-\infty}^{\infty} \frac{\mathrm{d}}{\mathrm{d}\zeta}|\hat{\phi}(\zeta)|^2\exp(-ij\zeta)\,\mathrm{d}\zeta \\ &= \frac{i}{4\pi(m_0 m_2)}\int_0^{2\pi} \frac{\mathrm{d}}{\mathrm{d}\zeta}\left(\sum_{k=-\infty}^{\infty}|\hat{\phi}(\zeta+2\pi k)|^2\right)\exp(-ij\zeta)\,\mathrm{d}\zeta = 0 \end{aligned} \tag{128}$$

Example 5.4. Here we adopt the procedure that is used by Battle [26], Lemarié [27], Meyer [19] and Chui [15] to construct orthogonal window functions.

[‡‡] It is believed that they can form a non-orthogonal wavelet basis in $L^2(\mathbb{R})$ under certain provisions; the detailed proof of the matter will be reported elsewhere

Choose a symmetric window function, $\phi(x)$, with reasonable decay at infinity and consider an orthogonal window function defined as

$$\hat{\phi}^*(\zeta) = \frac{\hat{\phi}(\zeta)}{\sqrt{\sum_{k=-\infty}^{\infty} |\hat{\phi}(\zeta + 2\pi k)|^2}} = \left(\sum_j \alpha_j \exp(-ij\zeta) \right) \hat{\phi}(\zeta) \tag{129}$$

Consequently, $\phi^*(x) = \sum_j \alpha_j \phi(x - j)$, where

$$\alpha_j = \frac{1}{2\pi} \int_0^{2\pi} \frac{\exp(-ijx)}{\sqrt{\sum_{k=-\infty}^{\infty} |\hat{\phi}(\zeta + 2\pi k)|^2}} \, \mathrm{d}x \tag{130}$$

Obviously, $\sum_k |\hat{\phi}^*(\zeta + 2\pi k)|^2 = 1$. The symmetry condition assures that $\hat{\phi}(\zeta)$ is real. Hence, the desired wavelet packets are

$$\psi_1^{[0]}(x) = m_0^{-1} \phi^*(x) = m_0^{-1} \sum_j \alpha_j \phi(x - j) \tag{131}$$

$$\psi_1^{[1]}(x) = m_2^{-1} x \phi^*(x) = m_2^{-1} \sum_j \alpha_j x \phi(x - j) \tag{132}$$

Numerical calculations have been carried out for both linear B-spline and the cubic spline functions. By definition

$$\hat{\phi}_1(\zeta) = \left(\frac{\sin(\zeta/2)}{\zeta/2} \right)^2 \quad \text{and} \quad \hat{\phi}_3(\zeta) = \left(\frac{\sin(\zeta/2)}{\zeta/2} \right)^4 \tag{133}$$

and subsequently (see [19, p. 62] for details),

$$\sum_{k=-\infty}^{\infty} |\hat{\phi}_1(\zeta + 2\pi k)|^2 = \frac{1}{3} + \frac{2}{3} \cos^2 \left(\frac{\zeta}{2} \right) =: P_4 \left(\cos \left(\frac{\zeta}{2} \right) \right) \tag{134}$$

$$\sum_{k=-\infty}^{\infty} |\hat{\phi}_3(\zeta + 2\pi k)|^2 = \frac{17}{315} - \frac{34}{315} \cos^8 \left(\frac{\zeta}{2} \right) + \frac{72}{315} \cos^6 \left(\frac{\zeta}{2} \right) + \frac{4}{105} \cos^4 \left(\frac{\zeta}{2} \right) + \frac{248}{315} \cos^2 \left(\frac{\zeta}{2} \right) =: P_8 \left(\cos \left(\frac{\zeta}{2} \right) \right) \tag{135}$$

Then

$$\hat{\phi}_1^*(\zeta) = \left(\frac{\sin(\zeta/2)}{\zeta/2} \right)^2 (P_4(\cos(\zeta/2)))^{-1/2} \tag{136}$$

$$\hat{\phi}_3^*(\zeta) = \left(\frac{\sin(\zeta/2)}{\zeta/2} \right)^4 (P_8(\cos(\zeta/2)))^{-1/2} \tag{137}$$

Substituting (134), (135) into (130), one may find α_j. Subsequently, the symmetric, orthonormal window function can then be found. By virtue of (131) and (132), one obtains the desired wavelet packet. Two orthogonal wavelet packets, which are with respect to linear B-spline and cubic spline

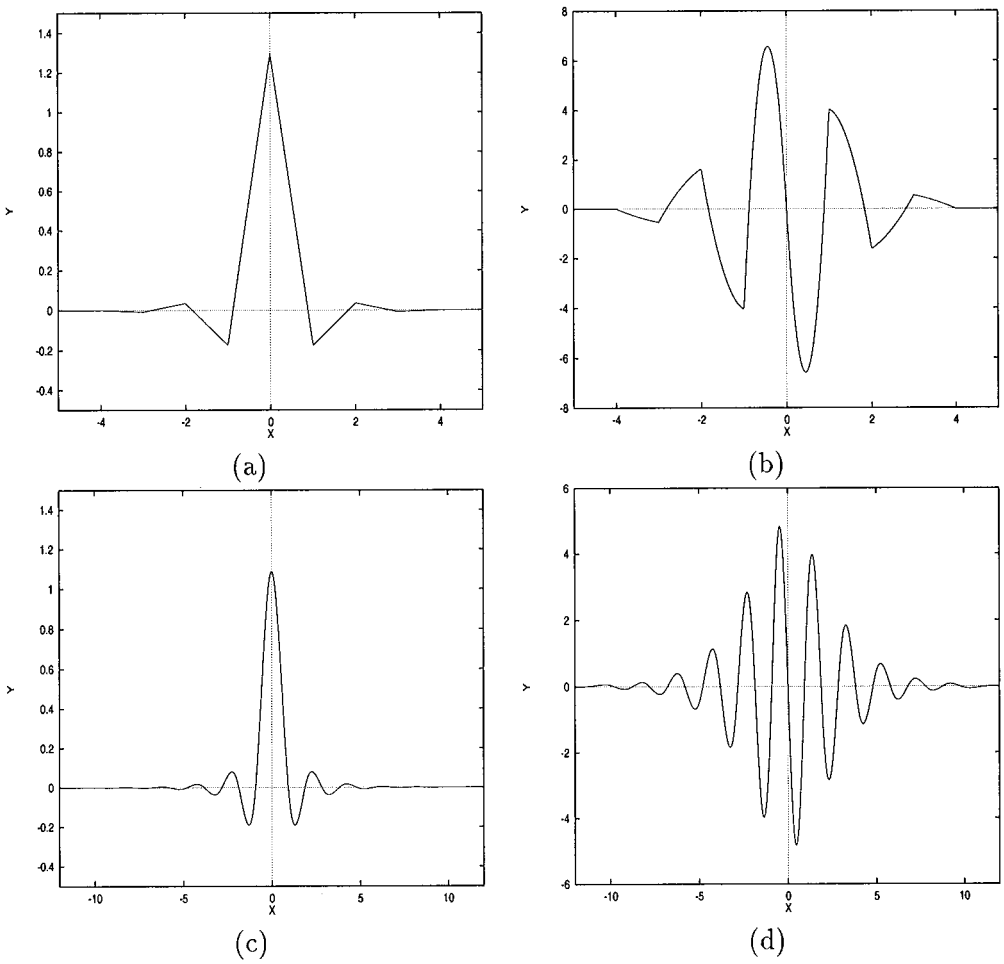

Figure 9. Orthogonal wavelet packets: (a) $\psi_1^{[0]}(x)$ w.r.t. $\phi_1(x)$, (b) $\psi_1^{[1]}(x)$ w.r.t. $\phi_1(x)$; (c) $\psi_1^{[0]}(x)$ w.r.t. $\phi_3(x)$, (d) $\psi_1^{[1]}$ w.r.t. $\phi_3(x)$

correspondingly, are displayed in Figure 9. The components of the wavelet packets generated here indeed form an orthogonal basis to each other.

Example 5.5. The pre-wavelet packet is generated based on a 2-D linear B-spline, $\phi_{2\mathrm{d}}(x_1,x_2)=\phi(x_1)\phi(x_2)$, and

$$\phi(x_i)=\begin{cases}1-|x_i|, & |x_i|\leqslant 1\\ 0 & \text{otherwise}\end{cases} \tag{138}$$

Thereby, the continuous wavelet packet can be expressed as $\psi_{2\mathrm{d}}^{[\alpha]}(x)=\mathbf{P}(x)\mathbf{b}^{(\alpha)}\phi_{2\mathrm{d}}(x)$, and $x=(x_1,x_2)$, $\alpha=(0,0),(1,0),(0,1)$. After solving vector, $\mathbf{b}^{(\alpha)}$, one may have explicit expression

$$\psi_{2\mathrm{d}}^{[0,0]}(x_1,x_2)=m_0^{-1}\phi_{2\mathrm{d}}(x_1,x_2) \tag{139}$$

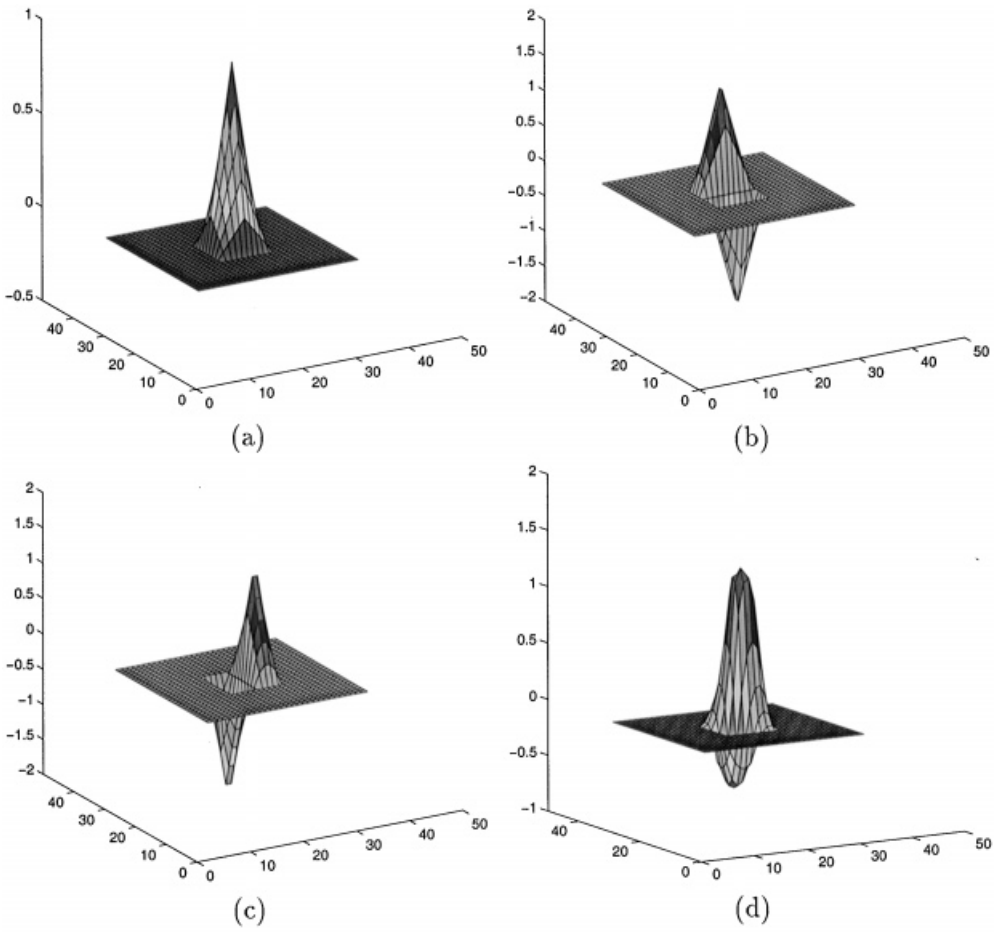

Figure 10. An 2-D wavelet kernel packets based on linear spline box: (a) $\psi_{2d}^{[0,0]}(x_1,x_2)$, (b) $\psi_{2d}^{[1,0]}(x_1,x_2)$; (c) $\psi_{2d}^{[0,1]}(x_1,x_2)$, (d) $\mathscr{K}_{2d}^{[s]}(x_1,x_2)$

$$\psi_{2d}^{[1,0]}(x_1,x_2) = m_{11}^{-1}x_1\phi_{2d}(x_1,x_2) \tag{140}$$

$$\psi_{2d}^{[0,1]}(x_1,x_2) = m_{22}^{-1}x_2\phi_{2d}(x_1,x_2) \tag{141}$$

Choose a direction $\mathbf{n} = (n_1, n_2)$. A synchronized reproducing kernel interpolant along $\mathbf{n}$ can be formed,

$$\mathscr{K}_{2d}^{[s]}(x) = \psi_{2d}^{[0,0]}(x) + \tau(n_1\psi_{2d}^{[1,0]}(x) + n_2\psi_{2d}^{[0,1]}(x)) \tag{142}$$

The 2-D wavelet kernel packet are depicted in Figures 10(a)–(c), and a synchronized reproducing kernel interpolant is shown in Figure 10(d) based on expression (142) with $\tau = 0{\cdot}5$ and $n_1 = n_2 = \cos(\pi/4)$.

6. CONCLUDING REMARKS

In the paper, we present a new meshless hierarchical partition of unity and the associated reproducing kernel formula, which is the consequence of the *discovery* of wavelet partition of nullity. We have shown here, as Liu and Chen [28] pointed out eariler, that there is a link between wavelet method and moving least square based reproducing kernel formula.

Moreover, the wavelet hierarchical partition of unity developed here may enable us to perform some special numerical operations, such as the p adaptivity refinement; multiple scale analysis; wavelet Petrov–Galerkin algorithm; and among others. These applications will be discussed in the Part II [29] of this work. We would like to note that the approximation theory of the reproducing kernel particle method presented here, and in [10] as well, is only for the cases that are involved with compact supported window functions. Recently, we found that some convergence results of the moving least-squares method for general window functions, which were given early by Farwig [30].

ACKNOWLEDGEMENTS

The material presented in this paper is mainly from the first author's (SL) Ph.D. dissertation [31]. This work is supported by grants from the Office of Naval Research, the Army Research Office, and National Science Foundations, and Tull Family Endowment Fund. The first author (SL) is also supported by Graham-Cabell fellowship from Northwestern University. This work is also sponsored in part by the Army High Performance Computing Research Center under the auspices of the Department of the Army, Army Research Laboratory cooperative agreement number DAAH04-95-2-003/contract number DAAH04-95-C-0008, the content of which does not necessarily reflect the position or the policy of the government, and no official endorsement should be inferred. The authors would like to thank Mr. Thomas Black for his careful reading of the manuscript and valuable comments and suggestions.

REFERENCES

1. Belytschko T, Krongauz Y, Organ D, Fleming M, Krysl P. Meshless methods: an overview and recent developments. *Computer Methods in Applied Mechanics and Engineering* 1996;**139**:3–48.
2. Liu WK, Chen Y, Uras RA, Chang CT. Generalized multiple scale reproducing kernel particle methods. *Computer Methods in Applied Mechanics and Engineering* 1996;**139**:91–158.
3. Melenk JM, Babuška I. The partition of unity finite element method: basic theory and applications. *Computer Methods in Applied Mechanics and Engineering* 1996;**139**:289–314.
4. Duarte CA, Oden JT. An hp adaptive method using clouds. *Computer Methods in Applied Mechanics and Engineering* 1996;**139**:237–262.
5. Duarte CA, Oden JT. *Hp* clouds — an hp meshless method. *Numerical Methods for Partial Differential Equations* 1996;**12**:673–705.
6. Taylor RL. Hierarchical partition of unity methods. In *4th U.S. National Congress on Computational Mechanics.* San Francisco, CA, 1997.
7. Zienkiewicz OC, de SR Gago JP, Kelly DW. The hierarchical concept in finite element analysis. *Computers and Structures* 1982;53–65.
8. Bank RE. Hierarchical bases and the finite element method. *Acta Numerica*; Cambridge University Press: Cambridge, 1996;1–43.
9. Lancaster P, Salkauskas K. Surface generated by moving least square methods. *Mathematics of Computation* 1980;**37**:141–158.
10. Liu WK, Li S, Belytschko T. Moving least square reproducing kernel method, Part 1: methodology and convergence. *Computer Methods in Applied Mechanics and Engineering* 1997;**143**:422–433.
11. Yang H. *Wave Packet and their Bifurcations in Geophysical Fluid Dynamics*; Springer: New York, 1990.
12. Coifman R, Meyer Y. Othogonormal wavelet packet bases. *Preprint*, Yale University, New Haven, CT, 1990.

13. Chui CK, Li C. Nonorthogonal wavelet packets. *SIAM Journal on Mathematical Analysis* 1993;**24**:712–755.
14. Duval-Destin M, Muschietti MA, Torresani B. Continuous wavelet decompositions, multiresolution, and contrast analysis. *SIAM Journal on Mathematics Analysis* 1993;**24**:739–755.
15. Chui CK. *An Introduction to Wavelets*; Academic Press: Boston, 1992.
16. Daubechies I. *Ten Lectures on Wavelets.* Philadelphia, PA: Society for Industrial and Applied Mathematics, 1992.
17. Szabó B, Babuška I. *Finite Element Analysis*; Wiley: New York, 1991.
18. Grossmann A, Morlet J. Decomposition of hardy function into square integrable wavelets of constant shape. *SIAM Journal of Mathematical Analysis* 1984;**15**:723–736.
19. Meyer Y. *Wavelets and Operators*; Cambridge University Press: Cambridge, 1992. The French edition was published in 1990 under the name *Ondelettes et Operateurs*.
20. Meyer Y, Ryan RD. *Wavelets: Algorithms & Applications*; SIAM: Philadelphia, 1993.
21. Kaiser G. *A Friendly Guide to Wavelets*; Birkhäuser: Boston, 1994.
22. Daubechies I. Orthonormal bases of compactly supported wavelets ii variations on a theme. *SIAM Journal on Mathematical Analysis* 1993;**24**:499–519.
23. Beylkin G, Coifman R, Rokhlin V. Fast wavelet transforms and numerical algorithm i, *Communications on Pure and Applied Mathematics* 1991;**XLIV**:141–183.
24. Delves L, Mohamed J. *Computational Methods for Integral Equations*; Cambridge University Press: New York, 1985.
25. Liu WK, Jun S, Zhang S. Reproducing kernel particle methods. *International Journal of Numerical Methods in Fluids* 1995;**20**:1081–1106.
26. Battle G. A block spin construction of ondelettes, Part 1: Lemarié functions. *Communications in Mathematical Physics* 1987;**110**:601–615.
27. Lemarié PG. Une nouvelle base dóndelettes de $l^2(\mathbb{R}^n)$. *Journal Mathematiques Pures et Appliques* 1988;**67**:227–236.
28. Liu WK, Chen Y. Wavelet and multiple scale reproducing kernel method. *International Journal of Numerical Methods in Fluids* 1995;**21**:901–933.
29. Li S, Liu WK. Reproducing kernel hierarchical partition of unity, Part ii: applications. *International Journal for Numerical Methods in Engineering* 1998.
30. Farwig R. Multivariate interpolation of arbitraily spaced data by moving least squares methods. *Journal of Computational and Applied Mathematics* 1986;**16**:79–93.
31. Li S. Moving least square reproducing kernel methods. Ph.D. Thesis, McCormick School of Engineering and Applied Science, Northwestern University, Evanston, IL, May 1997.

